THE IMPACT OF REDOX CONDITIONS ON OH• SCAVENGING IN SURFACE WATER MATRIX AND IMPLICATIONS FOR TESTING OF SCAVENGING

by

Jenny Nguyen

A thesis submitted to the faculty of
The University of North Carolina at Charlotte
in partial fulfillment of the requirements
for the degree of Master of Science in
Civil Engineering

Charlotte

2022

Approved by:

_____
Dr. Olya Keen

_____
Dr. James Amburgey

_____
Dr. Mei Sun

ABSTRACT

JENNY NGUYEN. The impact of redox conditions on $OH^{\bullet}$ scavenging in surface water matrix and implications for testing of scavenging (Under the direction of DR. OLYA KEEN)

Advanced oxidation processes (AOPs) in water treatment utilizes chemical oxidation to react with and promote the degradation of trace contaminants present in wastewater. Hydroxyl radicals ($OH^{\bullet}$) generated in AOPs are highly reactive and nonselective, capable of targeting these trace contaminants. Background water constituents like bicarbonate, carbonate, and dissolved organic matter (DOC) are termed hydroxyl radical scavengers that will compete with these trace contaminants and decrease the effectiveness of AOPs. In AOP testing for scavenging, DOC is interpreted as a bulk parameter where an average reaction rate constant has been reported and used. This interpretation can provide inaccurate scavenging predictions as there is a wide range of variability in reaction rate constants between organic compounds and $OH^{\bullet}$. Therefore, measurement of scavenging is a preferred approach, however there is currently no guidance in literature on handling of such samples. Scavenging was quantified for water samples from two surface water sources (Concord and Mount Holly) over the course of two seasons at different hold times and storage conditions using a bench-scale collimated beam UV design with a low-pressure lamp. Samples were stored with headspace space and no headspace after collection and scavenging was analyzed at hold times of 0 HR, 24 HR, 48 HR, 7 HR, 7 days and 14 days. Results reveal that 52% of all measured scavenging significantly ($\alpha = 0.05$) drifted compared to initial day scavenging indicating that testing should be within 24 HR of hold time. Furthermore, 69% of all headspace

samples drifted while 63% of no headspace samples drifted. Concord samples revealed significant differences in storage conditions for all winter samples analyzed ($\alpha = 0.05$), however no differences in the summer samples. Mount Holly samples revealed significant differences in both winter and summer seasons ($\alpha = 0.05$). As a result, samples should be stored with no headspace for testing to preserve the sample as much as possible. Additionally, as reactions with $OH^{\bullet}$ are oxidation reactions, the oxidation state of carbon was calculated for over 1,000 organic compounds and correlated with their respective reaction rate constants with $OH^{\bullet}$ to study the relationship between the two variables. Results show that reaction rate constants with $OH^{\bullet}$ between organic compounds with positive versus negative oxidation states of carbon is significantly different with a p-value of 0.0000204 ($\alpha = 0.05$), thus drawing the conclusion that reaction rates are influenced by the average oxidation state of carbon. Additionally, negative versus zero oxidation states of carbon yielded a p-value of 0.000818 ($\alpha = 0.05$). The results of the experiments with the surface water samples confirmed that the redox condition of the sample measured as oxidation-reduction potential (ORP) has influence on the reaction rate of dissolved organic matter with hydroxyl radicals, possibly by changing the redox state of the carbon on dissolved organic matter. However, the trends were localized for some sample sets and no universal trend was observed for all water samples. The results also highlight the variability of scavenging rates attributable to dissolved organic matter and emphasize the importance of experimental measurement of scavenging rather than calculation based on water quality parameters.

ACKNOWLEDGEMENTS

I would like to give a big thank you to my advisor, Dr. Olya Keen for her support since the very start of my graduate journey. It has been academically challenging but extremely rewarding thanks to her passion that inspired me to push through my research. I would like to also thank my thesis committee, Dr. James Amburgey and Dr. Mei Sun for their insightful feedback and guidance on improving my research.

Thank you to my parents for the love and support every day as I navigated this journey. Thank you to my close friends who always listened to my research related conversations/rants and still gave me the best encouragements every time.

TABLE OF CONTENTS

LIST OF TABLES

LIST OF FIGURES

ABBREVIATIONS

AOP	advanced oxidation process
CH_4	methane
CO_2	carbon dioxide
DOC	dissolved organic carbon
DOM	dissolved organic matter
H_2O_2	hydrogen peroxide
HS	headspace
HS^-	bisulfide
$KMnO_4$	potassium permanganate
MB	methylene blue
NOM	natural organic matter
NOSC	nominal oxidation state of carbon
NPOC	non-purgeable organic carbon
O3	ozone
$OH^\bullet$	hydroxyl radical
ORP	oxidation reduction potential
ROS	reactive oxygen species
TOC	total organic carbon
UV	ultra-violet

CHAPTER 1: INTRODUCTION

1.1 Advanced Oxidation Processes

Advanced oxidation processes (AOPs) are a water and wastewater treatment method that utilizes chemical oxidation to remove organic and inorganic pollutants. This practice was first introduced in the 1980s as a treatment option for potable water before being implemented in wastewater treatment (Deng and Zhao, 2015). Powerful oxidizing radicals are generated in AOPs to oxidize and degrade organic and inorganic pollutants into more stable harmless forms, while increasing water biodegradability overall for further treatment (Sarathy et al., 2011; Deng and Zhao, 2015).

AOPs generate hydroxyl radicals ($OH^{\bullet}$) through several different methods. These methods include treatment that are ozone-based, ultraviolet (UV) light-based, hydrogen peroxide (H_2O_2)-based, Fenton-based or a combination of methods depending on wastewater characteristics and the economic feasibility (Dong et al., 2010; Deng and Zhao, 2015). Among the different methods, different techniques can be utilized to produce these radicals such as irradiation, use of catalysts, or in conjunction with other oxidizing agents (Deng and Zhao, 2015; Gligorovski et al., 2015). Through the technique of irradiation, $OH^{\bullet}$ can be produced by photolysis with UV light exposure where H_2O_2 molecules split into two $OH^{\bullet}$ in aqueous solutions (Brezonik et al., 1988; Souza et al., 2013; Deng and Zhao, 2015; Gligorovski et al., 2015). The use of other oxidizing agents includes ozone (O_3) where two molecules of $OH^{\bullet}$ can be produced from three O_3 molecules under specific conditions (Deng and Zhao, 2015). Lastly, in Fenton-based

AOPs the presence of catalysts such as iron (Fe^{2+}/Fe^{3+}) with H_2O_2 can produce $OH^{\bullet}$ in aqueous solutions (Deng and Zhao, 2015; Gligorovski et al., 2015).

1.2 Hydroxyl Radicals

Hydroxyl radicals are considered one of the most important oxidizing agents in water treatment, with the highest oxidation-potential between +2.8 V to +1.95 V (Deng and Zhao, 2015; Gligorovski et al., 2015). These radicals belong to a class of reactive oxygen species (ROS), capable of reacting with compounds at rates between 10^8 - 10^{10} M^{-1} s^{-1} and behave non-selectively towards pollutants (Buxton et al., 1987; Deng and Zhao, 2015; Gligorovski et al., 2015).

Reactions with $OH^{\bullet}$ are described as diffusion-controlled reactions where reactivity is dependent upon how quickly the radical can encounter a molecule. As the radical reacts with a compound, it can attack in several ways: by radical addition, hydrogen abstraction, electron transfer, or radical combination (Brezonik et al., 1998; Deng and Zhao, 2015). With radical addition, the $OH^{\bullet}$ will attach to a carbon-carbon unsaturated bond (C=C) or via an aromatic ring substitution (Gligorovski et al., 2015). With hydrogen abstraction, the $OH^{\bullet}$ can target compounds by stealing hydrogen (H) atoms to form water molecules (Gligorovski et al., 2015). Electron transfer refers to the mechanism involved in oxidation-reduction reactions where an oxidizing agent gains electrons from reduced compounds. $OH^{\bullet}$ are oxidizing agents and therefore will accept electrons from reduced chemical species via electron transfer.

1.3 Hydroxyl Radical Scavenging

AOP treatment efficiency can be greatly reduced by $OH^{\bullet}$ scavengers, primarily constituents such as natural organic matter (NOM), bicarbonate, and carbonate species naturally abundant in water (Brezonik et al., 1998; Dong et al., 2010). NOM is a general term to define a complex mixture of organic compounds of varying molecular structure and molecular weight, (Sharp et al., 2006), where NOM and other natural constituents collectively behave as oxidant scavengers that will react with $OH^{\bullet}$ directly and decrease the effectiveness of treatment towards target organic pollutants or trace contaminants. Due to this, treatment facilities must understand $OH^{\bullet}$ consumption directly from scavengers versus $OH^{\bullet}$ generation to optimize AOP efficiency. However, as water composition can vary significantly from source to source or even within the same source daily, $OH^{\bullet}$ scavenging can be difficult to predict and quantify. The known concentration of NOM quantified as dissolved organic carbon (DOC) can be related to the scavenging activity of $OH^{\bullet}$ (Westeroff et al., 1998), however NOM is interpreted as a bulk parameter in AOP modeling and thus an assumed constant derived from organic matter isolates or specific organic matter groups have been used to estimate performance. Several reported values have reported an average second-order rate constant between $OH^{\bullet}$ and NOM ranging from 1.9×10^4 L mg-$C^{-1}s^{-1}$ (Goldstone et al., 2002) to 3×10^4 L mg-$C^{-1}s^{-1}$ (Westeroff et al., 1998).

The nature of NOM varies in terms of structure and composition depending on source water, therefore quantifying NOM as a bulk parameter could inaccurately predict AOP performance. Over 1,200 described reaction rates between organic compounds and $OH^{\bullet}$ has been investigated by Buxton et al. (1987) to highlight the wide range of

reactivity rates. Furthermore, numerous studies have investigated the potential factors and characteristics of NOM such as compound structure (Westeroff et al, 1998; Xican Li., 2013), functional groups (Yang et al., 2010), and even molecular weight (Dong et al., 2010) that could potentially influence reactivity rates.

1.4 Oxidation State of Carbon

Despite published studies exploring multiple factors that affect $OH^{\bullet}$ scavenging, a gap in the literature exists about whether oxidation state of carbon influences scavenging. The oxidation state of carbon can be described as the net charge of an atom which increases as the degree of lost electrons increases while bonded to more electronegative atoms, and the net charge decreases as the degree of gained electrons increases while boned to less electronegative atoms (Kroll et al., 2011). For carbon atoms, the oxidation state can range from a very reduced state of -4 seen in compounds such as methane (CH_4), to a very oxidized state of +4 seen in compounds of carbon dioxide (CO_2). The average oxidation state of carbon is often described for carbon containing organic compounds with a number of carbon atoms. In this situation, the oxidation state of individual carbons can be calculated based on what is bonded to it, where the overall average oxidation state of carbon for that molecule can be determined. This research aims to understand whether the average oxidation state of carbon in organic compounds directly influence reactivity with $OH^{\bullet}$. Because reactions with $OH^{\bullet}$ are oxidation reactions, reduced carbon should react more readily with an oxidant like $OH^{\bullet}$ compared to oxidized carbon.

1.5 Oxidation-Reduction Potential

A limited number of studies have linked the relationship between environmental redox conditions and the direct changes on organic carbon oxidation states (discussed further in Chapter 3), however this research aims to further expand on this with the notion that the subsequent change in carbon oxidation state due to the environment could allow for favorable or unfavorable scavenging conditions. Oxidation-reduction potential (ORP) quantifies the oxidizing or reducing intensity of a system, which in this study will be aqueous solutions (EPA, 2022). The general term oxidation implies the tendency for atoms to lose electrons and reduction implies the tendency for atoms to gain electrons. In aqueous solutions, the ORP quantifies whether the chemical species within the matrix are at a greater affinity for gaining electrons or losing electrons from new chemical species if they were introduced (EPA, 2022). An electrode probe is used to measure the ORP of a solution in unit measurements of millivolts (mV). Positive millivolts imply the intensity of oxidizing conditions and negative millivolts implies the intensity of reduced conditions.

1.6 Research Objective

Reactions involving $OH^{\bullet}$ is an oxidation reaction, meaning the more reduced a molecule is, the more readily oxidized it will be. The foundation of this relationship will provide the framework to experimentally determine how environmental ORP influences scavenging of $OH^{\bullet}$ by organic matter. If significant, this research can give insight on specific conditions that would decrease or encourage scavenging from organic matter,

which would translate advantageously for predicting AOP performance. The following section outlines the objectives, experimental tasks, and hypothesis for this research.

- Objectives
    - Investigate how environmental redox conditions can affect the oxidation state of carbon in organic matter through literature review.
    - Investigate the effect of the average oxidation state of carbon on the reaction rate of the compound with $OH^{\bullet}$
    - Determine the effect of ORP on the measured scavenging of $OH^{\bullet}$ and provide recommendations for sample handling and storage to improve testing of scavenging for AOP.

- Research Tasks
    - Determine statistically (t-Test) whether the average carbon oxidation state has a significant impact on the reactivity of an organic molecule with $OH^{\bullet}$ by examining rate constants for compounds with different average carbon oxidation state.
    - Experimentally and statistically (t-Test) analyze the effects of scavenging of $OH^{\bullet}$ at different hold times.
        - Determine whether the $OH^{\bullet}$ scavenging remains relatively constant or changes significantly over a course of specific hold times and how ORP changes over time influence scavenging
        - In theory, allowing samples stored with headspace or oxygen present will allow the system to become more oxidized as oxygen

is an oxidizer and scavenging would decrease. Alternatively, storing samples without headspace or oxygen absent, will allow the system to become more reduced and scavenging would increase. Measured scavenging for both sets of samples to evaluate the differences.

- Establish appropriate hold time by experimentally analyzing the samples on collection day, and then headspace and no-headspace samples at 24 hours, 48 hours, 72 hours, 7 days, and 14 days after collection day.

- Experimentally and statistically analyze the ORP of samples stored with headspace and without headspace.
- Determine statistically whether the ORP, measured $OH^{\bullet}$ scavenging, and calculated DOC rate constants for reaction with $OH^{\bullet}$ are significantly different between headspace and no headspace storage conditions, and whether ORP can predict the changes in DOC rate constant.

- Hypothesis
  - Hypothesis I: Carbon oxidation state will influence the reactivity between organic compounds and $OH^{\bullet}$. Average reduced state of carbon will have higher rate constants with $OH^{\bullet}$ while the average oxidized state of carbon will have lower rate constants with $OH^{\bullet}$.
  - Hypothesis II: The ORP of the water matrix will influence $OH^{\bullet}$ scavenging by organic matter. In reducing conditions, scavenging is expected to

increase and in more oxidizing conditions, scavenging is expected to decrease.

1.7 Research Approach

A relationship between the nominal oxidation state of carbon (NOSC) (LaRowe et al., 2018) of organic compounds and the reaction rates of $OH^{\bullet}$ is first evaluated to determine if there is a significant difference in reactivity with $OH^{\bullet}$ between positive and negative NOSC. This will set the foundation for the next portion of the research by correlating the relationship between ORP and $OH^{\bullet}$ scavenging changes in surface water at different hold times and storage conditions. Results are then processed and statistically analyzed for differences and correlations to test the hypotheses and objectives summarized in the previous section.

CHAPTER 2: LITERATURE REVIEW

2.1 Environment ORP and Organic Matter

2.1.1 Quinone and Hydroquinone Moieties

There have been several studies documenting the influence of changing environmental redox conditions on organic matter, although more limited on the oxidation state of carbon specifically. According to literature, changes in organic compounds within humic substances due to the changing environment can be attributed to quinone-hydroquinone moieties as they are described as redox-active (Aeschbacher et al., 2009; Kane et al., 2019; Peng et al., 2022). For example, in changing redox conditions within capillary fringes of soil, redox-active moieties in humic substances behave as redox buffers by either accepting electrons under anoxic conditions or donating electrons in aerobic conditions (Aeschbacher et al., 2010; Stern et al., 2018). This allows the system to become more reduced under anoxic conditions and more oxidized under aerobic conditions.

Kane et al., (2019) further investigated the effects of plant groups present with changing water table positions in soil profiles on the redox conditions of the environment and the redox activity of phenolics in DOM. It was concluded that these factors interact interchangeably. Changing redox conditions changed the chemical and physical properties of DOM where phenolics of higher molecular weight were more readily oxidized depending on certain redox conditions. It was also stated that the electron accepting capacity of humic substances increases relative to quinone or quinone-like content in phenolic DOM, supporting a number of other studies on the redox role of these moieties.

Furthermore, the nominal oxidation state of carbon (NOSC) influences the decomposability in DOM in low oxygen environments (Boye et al., 2017). With low NOSC DOM in reducing environments, the energy required to fully oxidize DOM is expected to increase as it becomes more thermodynamically unfavorable (Keiluweit et al., 2016; Dick et al., 2019). Kane et al., (2019) have investigated that low average NOSC of carbon in anoxic reducing conditions is contributed by low thermodynamically favorable conditions to oxidize carbon, similar to research from Boyle et al., (2017), Dick et al., (2019) and Keiluweit et al., (2016), where low energetic constraints resulted in the disabling of microbial metabolic activity to oxidize reduced organic carbon compounds.

2.1.2 Redox Gradients and Carbon Oxidation State

A study done by Dick et al., (2019) have linked the impact of environmental redox changes on DNA proteins, more specifically how the genome of organisms responds to the geochemistry changes in the environment by analyzing the carbon redox state. This research demonstrated that the carbon oxidation state of natural organic matter is linked to changing environmental conditions and investigated the influence of marine and terrestrial redox gradients on the carbon oxidation state in DNA and proteins. The reasoning for these changes boils down to thermodynamic constraints that redox gradients exert on the biomacromolecules.

The NOSC range for DNA and proteins are small but found that the oxidation state of carbon increases in highly oxic surface waters in many environments. Other samples have demonstrated that the NOSC increases towards cooler oxidizing conditions in environments such as Diffuse Vents, hydrothermal vents, the Shin-Yan-Ny-Hu Mud

Volcano in Taiwan, Organic Lake in Antarctica, serpentine springs, and Yellowstone Park (Dick et al., 2019). In Baltic Sea sediments, the NOSC of DNA is observed to decrease from the surface down to 41-42 meters below seafloor towards reducing conditions where electron acceptors are depleted and anaerobic microbial activities such as methanogenesis are occurring (Dick et al., 2019).

Although these relationships can be attributed as a consequence of thermodynamic constraints, it was not dominant in all redox gradients. One condition where the thermodynamic constraint model was not applicable is in marine oxygen minimum zones where carbon oxidation states were negatively correlated with oxygen concentration and this was likely due to minimal nutrient availability and the genome adaptability of microorganisms as a result Dick et al., (2019).

2.2 Factors Impacting $OH^{\bullet}$ Scavenging

2.2.1 Structure of NOM and Scavenging

Compound structures like bonds have been shown to influence reactivity in several studies. $OH^{\bullet}$ tends to react quicker with carbon-carbon double (C=C) and triple bonds over carbon-carbon single or carbon-hydrogen bonds (Westeroff et al., 1998). Another study done by Xican Li, (2013) supports this behavior where it was observed that n-Hexane and petroleum ether (hydrocarbons) containing only C-H or C-C sigma bonds are more stable and resistant to $OH^{\bullet}$ attacks. Furthermore, moderate scavenging was observed from cyclohexane, benzene, toluene, carbon tetrachloride, chloroform, dichloromethane due to molecules containing conjugated π bonds and polar carbon-halogen Σ bonds (Xican Li, 2013). Strong scavenging was observed from acetonitrile,

acetone, and carbon disulphide due to non-conjugated unsaturated bonds (C≡N, C=O, C=S), and the strongest $OH^{\bullet}$ scavenging observed came from diethyl ether, DMF, DMSO, ethanol, ethyl acetate, methanol and THF (Xican Li, 2013). In these compounds, at least one oxygen atom was present to form carbon-oxygen bonds, hydrogen-oxygen bonds, or sulfur-oxygen double bonds, and consists of hydroxyl, ester, amide, sulfinyl, or cyclic ether functional groups (Xican Li, 2013). Among specific functional groups, a study done by Yang et al. (2010) observed that the amino group, acetamide group, and hydroxyl group have the highest to lowest $OH^{\bullet}$ scavenging activity respectively (Yang et al., 2010).

2.2.2 Molecular Weight of Organic Matter and Scavenging

A study done by Dong et al. (2010) analyzed the relationship between effluent organic matter with $OH^{\bullet}$ to suggest how reaction rates change as a function of molecular weight. It was concluded that as the apparent molecular weight increases, the reaction rate between effluent organic matter and $OH^{\bullet}$ decreases due to the fact that the 3-D configuration becomes highly aggregated and complex as molecular weight increases, making individual carbon atoms less accessible to $OH^{\bullet}$. Since reactions with $OH^{\bullet}$ are described as diffusion-controlled, this would make sense as rates can be influenced by how fast the radical reaches a particular atom or group.

2.2.3 Carbon Number and Scavenging

A study by Arakaki et al., (2013) helped improve the prediction of AOP performance by quantifying the scavenging of $OH^{\bullet}$ by organic matter as a product of dissolved organic carbon concentration (mol-C/L) and the general scavenging rate

constant in addition to the concentration of organic compounds (mol-compound/L) and the general scavenging rate constant. This study further evaluated the strength of these relationships by factoring in the number of carbon atoms in individual organic compounds and the rate constants with $OH^{\bullet}$ listed in Buxton et al., (1987). Results have shown that the relationship was not strong for small organic compounds but as the carbon number increases, the reactivity with $OH^{\bullet}$ increases to up to $10^{10}\ M^{-1}\ s^{-1}$ for both carbon concentration and organic compound concentration.

2.3 Carbon Oxidation State and Scavenging

By changing the redox conditions of the water matrix, this research will analyze how this affects the scavenging behavior between DOM with $OH^{\bullet}$. It is hypothesized that reaction rates between $OH^{\bullet}$ and organic compounds are positively correlated with carbon oxidation state. While several studies were investigated for this research that evaluates the relationship between $OH^{\bullet}$ reactivity with organic matter under different conditions, no research has linked the impact of $OH^{\bullet}$ reactivity based on carbon oxidation state. One study has linked the impact of $OH^{\bullet}$ reactivity under overall redox conditions of the water matrix. A study done by Souza et al., (2013) utilized the UV/H_2O_2 method to investigate $OH^{\bullet}$ scavenging and removal performance on the target compound atrazine and found that low oxidizing conditions and stability of the triazine ring structure did not allow for complete transformation to cyanuric acid, drawing a relationship between poor oxidation performance by $OH^{\bullet}$ attributing to redox conditions and molecular structure.

CHAPTER 3: MATERIALS AND METHODS

3.1 Sample Collection

Samples were collected from two different water treatment facilities: Concord, North Carolina and Mount Holly, North Carolina. Grab samples were collected after undergoing the general facility treatment process but before the addition of disinfectant to avoid any presence of oxidants that could interfere with laboratory procedures. It was important for this research to collect samples at treatment facilities that do not implement pretreatment using photosensitive oxidants such as chlorine in incoming raw water within their treatment process.

The Mount Holly water treatment facility draws water from a nearby reservoir called Mountain Island Lake, where it is injected with aluminum sulfate for the coagulation process before entering the rapid mix chambers. Treatment is then followed by flocculation, sedimentation, treated with a low dose of chlorine before filtration, and then goes through disinfection with a higher dose of chlorine. After disinfection, pH adjustment is initiated using caustic, phosphate is added for corrosion control, and hydrofluosilicic acid is added for cavity prevention. Samples at this facility were obtained immediately before any chlorine disinfectants were added.

The Concord water treatment facility pretreats raw incoming water with potassium permanganate to oxidize iron and manganese before adding powdered activated carbon to remove organics and reduce odor. Following pretreatment, coagulation using aluminum sulfate and flocculation using polymer is next, followed by filtration through dual-media gravity filters and then disinfected with sodium hypochlorite. Post treatment consists of pH adjustment with sodium hydroxide, fluoride

addition for cavity prevention, and polyphosphate addition for corrosion control before final discharge to the public. Samples were obtained after filtration.

About seven liters of water samples were collected in 1-L amber glass bottles for each event to allocate approximately one liter of sample for each day during a sampling course: Day 0 (initial collection day), 24-hours, 48-hours, 72-hours, 7-days, and 14 days. Sampling was done once during the winter season and once during the summer season for both sites to capture the water characteristics over a range of seasonal temperatures. DOM is reported to increase in fall/winter months and decrease in spring/summer months (Sharp et al., 2006). This is likely due to decreased microbial activity during winter, resulting in plant decay contributing to an increase in NOM levels.

3.2 Sample Preparation and Storage

3.2.1 Filtration

All water samples were placed directly into a chiller to prepare for filtration and first day sampling. The filtration apparatus includes a 300-mL glass funnel attached to a glass supported silicone base using an aluminum clamp and nestled into a 1000-mL receiver flask that is attached to a second 1000-mL vacuum suction flask via rubber tubing. A small amount of vacuum suction is then applied to the suction flask to allow the sample to filter through the 0.45-μm pore diameter glass fiber filter into the receiver flask. The filter is first rinsed with 1000 mL of deionized water and discarded before filtering the samples.

3.2.2 Headspace

Filtered samples are then allocated to be stored with headspace and without headspace. 500-mL of filtered headspace samples were allocated for each hold time by storing it in 1-L glass amber bottles and another 500-mL of filtered non-headspace samples were stored in two 250-mL amber bottles. All prepped samples were then placed back into the 4°C chiller and will remain until needed for testing. For each hold time, both headspace and non-headspace samples were analyzed in conjunction to evaluate the potential differences over time. On collection day (initial day samples) however, only one set of samples were analyzed as there are no hold time or headspace storage differences to evaluate. Initial day samples serve as a control or baseline to compare how data changes as factors such as hold time and headspace storage are implemented.

3.3 TOC Analyzer

Dissolved organic carbon is measured using the non-purgeable organic carbon (NPOC) method with a Shimadzu™ TOC-L Series Total Organic Carbon (TOC) Analyzer and a Shimadzu™ ASI-L Auto Sampler. In the NPOC process, the sample is acidified automatically with HCl to pH 3 where the sparging process starts to convert inorganic carbon and purgeable organic carbon to carbon dioxide and removed. The total carbon is then measured by pulling in purified air and undergoes combustion by heating to 680°C with a platinum catalyst. 40-mL glass screw-top vials were used in the TOC analyzer. For each testing day, DOC is measured for both headspace and no-headspace samples under one sampling session. For each sample measured, four 40-mL vials of

nanopure water are added to the analysis as blanks and washes. Nanopure water was obtained from a Taylor Scientific NANOpure Diamond™ water purification system.

For every 10-20 samples analyzed, TOC standards were prepared to ensure quality assurance and accuracy. Approximately 3-g of reagent grade white crystalline powder potassium hydrogen phthalate obtained from Alfa Aesar™ (Lot No. W21B030) was oven dried for 30 minutes at 110℃ and cooled for another 30 minutes in a desiccator. A stock solution of 400 mg-C/L was made by dissolving 2.125-g of the oven dried potassium hydrogen phthalate into 1-L of 18-MΩ water. The exact carbon concentration is then calculated from the following equation:

$$\frac{Mass\ of\ KHP\ added\ (g)}{Volume\ of\ Water\ (L)} \times 470.5 = Stock\ Concentration\ \left[\frac{mg-C}{L}\right] \quad (1)$$

Stock solution is kept in a 4℃ refrigerator and has a shelf life of one month. Standards of various concentrations are tested during the sampling session. Table 3-1 lists the stock volume to nanopure water needed for each standard in 40-mL vials.

Table 1: Stock to Nanopure Volumes for TOC Standards

Concentration (ppm)	Volume of Stock (μL)	Volume of Nanopure (mL)
0.2	20	39.98
0.3	30	39.97
0.5	50	39.95
1	100	39.9
2	200	39.8
3	300	39.7
5	500	39.5

Once testing is completed, the sample results are given as an average of three data points in mg-C/L. These results are used in the final scavenging calculations discussed in section 3.10.

3.4 Water Characteristics Measurements

Both the pH probe and ORP electrode are interchangeable probes that were used in conjunction with a Fisherbrand™ accumet™ AP125 Portable pH/Ion/mV/Temperature Meter, accumet AP125 Meter kit (Serial No. 837618) to measure water characteristics.

3.4.1 Measuring pH

The pH is measured using a Fisherbrand™ accumet™ pH/ATC Electrode for AP60 and AP100 Series Meters, Mercury-Free (Catalog No.13-620-AP50A). The probe is calibrated each testing day using pH 4.00, 7.00, and 10.00 buffer solutions from Fisher Chemical™. After calibration, the probe is dipped in a small beaker containing sufficient volume of the sample and readings are recorded once stabilized.

3.4.2 Measuring ORP

The ORP is measured in millivolts (mV) for each sample using a Fisherbrand™ accumet™ Metallic Ag/AgCl ORP Combination Electrode, Mercury-Free, with a platinum pin (Catalog No. 13-620-81). The electrode is placed directly into a small beaker containing sufficient volume of the sample and readings are recorded once stabilized. Calibration of the ORP probe involves dipping the probe direction into an

Thermo Scientific Orion™ 967901 ORP Standard 475-mL solution to get a redox potential value of +220 mV for the Ag/AgCl reference electrode.

3.4.3 Measuring Alkalinity

Alkalinity is measured for both sets of samples each day using an Alkalinity HACH™ Digital Titrator model AL-DT (Catalog No. 20637-00). One HACH™ pillow packet of bromocresol green-methyl red indicator powder was added to 100-mL of sample and swirled until evenly mixed. A digital titration cartridge of 0.16 N sulfuric acid was used to titrate the sample to a pH of 4.9 and the total number of digits (800 digits/mL or 0.00125 mL/digit) is recorded to be calculated as bicarbonate alkalinity or [HCO_3^-]. Calculations are as follows:

$$\text{Total Alkalinity (as } CaCO_3 \text{ in mg/L)} = \text{Bicarbonate Alkalinity (as } CaCO_3 \text{ in mg/L)} = (\text{Digit Multiplier}) \cdot (\#\text{ of digits to pH 4.9}) \quad (2)$$

$$\text{Bicarbonate Alkalinity (eq/L)} = [\text{Bicarbonate (as } CaCO_3 \text{ in mg/L)} \cdot 2 \text{ eq/mol}] \div (100{,}000 \text{ mg/mol } CaCO_3) \quad (3)$$

In Equation 2, for samples below a pH of 8.3 the phenolphthalein alkalinity equal 0 mg/L, therefore the total alkalinity is equal to bicarbonate alkalinity as $CaCO_3$. For Equation 3, bicarbonate in mg/L as $CaCO_3$ has an equivalent-to-equivalent ratio with [HCO_3^-] as 1:2, therefore a multiplication factor of 2 is needed. This product is then converted from mg/L as $CaCO_3$ to mol/L as Bicarbonate Alkalinity, where the molecular

weight of $CaCO_3$ is 100-g/mol or 100,000 mg/mol. The digit multiplier depends on the cartridge concentration of sulfuric acid used, where 0.16 N requires a digit multiplier of 0.1 and a cartridge of 1.6 N requires a digit multiplier of 1.

3.5 Reagents

This section summarizes the reagents and preparation procedures for this experiment. All stock solutions were kept chilled in a refrigerator at 4°C at all times.

3.5.1 Solution A

Solution A is a reagent used for preparing H_2O_2 measurements using the triiodide methodology adapted from Klassen et al., (1994) later discussed in section 3.6. To prepare Solution A stock solution, 36.67 g of 99% crystalline power potassium iodide manufactured by Alfa Aesar™, (Lot No. 10230183), 1.11 g of 97% reagent grade sodium hydroxide flakes manufactured by Sigma-Aldrich™ (Lot No. MKBS6981V), and 0.11 g of ammonium molybdate tetrahydrate (Lot No. BCBF7555V) manufactured by Fluka Analytical™ were dissolved in one-liter of deionized water and stored in a one-liter amber glass bottle. Molybdate is a heavy metal and must be disposed of as a hazardous waste. Solution A has a limited shelf life of about 6 months and will begin forming a yellow tint as it degrades that will interfere with readings. Frequent light exposure will accelerate the color change.

3.5.2 Solution B

Solution B is a second reagent used for preparing H_2O_2 measurements using the triiodide methodology adapted from Klassen et al., (1994) later discussed in section 3.6. To prepare Solution B, 11.11 g of reagent grade white crystalline powder potassium hydrogen phthalate obtained from Alfa Aesar™ (Lot No. W21B030) was dissolved in one liter of deionized water and stored in an amber glass bottle. This reagent is non-hazardous waste and can be disposed of safely down the drain.

3.5.3 Methylene Blue

Methylene blue (MB) is used as the probe compound in this study to assess $OH^{\bullet}$ generation through the decay of MB, further discussed in section 3.9. A stock solution concentration of 500-µM MB manufactured by J.T. Baker™ (CAS No. 7220-79-3) and stored in a one-liter amber glass bottle.

3.5.4 Hydrogen Peroxide

To prepare a stock solution of H_2O_2, 30% w/w aqueous H_2O_2 solution manufactured by J.T. Baker™ (Product No. 5846-03) is used. The density of the reagent is 1,110 g/L, with a concentration of approximately 333 g/L or 333,000 mg/L. To prepare a 100 mL stock solution with a concentration of 1000 mg/L, 0.3 mL of the 30% H_2O_2 stock is needed in 99.7 mL of deionized water. The reagent is then stored in a small amber glass bottle. H_2O_2 stock solution can begin to degrade overtime while in storage therefore a new stock solution is recommended when concentration begin to decrease despite using the same volume during testing.

3.6 Triiodide Methodology for H_2O_2 Measurement

The H_2O_2 concentration is measured by a user program created on a HACH DR6000 spectrophotometer using the triiodide method adapted from Klassen et al., (1994). Sample preparation involves portioning 160-mL of headspace and no-headspace samples in a 250-mL flask each and adding 0.267 mL of H_2O_2 stock solution into each. Flasks need to be swirled sufficiently to allow for a homogeneous mixture.

Before measurements, the spectrophotometer needs to be zeroed by adding 0.563 mL of Solution A and Solution B into one 1-cm quartz cuvette and zeroed. After zeroing, add 0.125 mL of the headspace H_2O_2 sample into the zeroed cuvette with the mixture of Solution A and Solution B. Ensure the solution within the cuvette is mixed adequately and wait for 60 seconds to allow triiodide to form from the molybdenum catalyzed reaction between iodide and H_2O_2. This method reads the absorbance of triiodide and converts the concentration to H_2O_2 in mg/L by multiplying it with a factor of 12.854 as the reaction of H_2O_2 to triiodide has a 1:1 mole ratio.

After 60 seconds, allow the spectrophotometer to read the H_2O_2 concentration. This method is repeated for both headspace and no-headspace samples until at least three readings are within ±0.5 mg/L to calculate an average for each.

3.7 Bench-Scale Collimated Beam UV System

The following UV system methodology was based from Bolton and Linden, (2003) and their protocol for bench scale UV experiments. The UV system used in this research is a quasi-collimated beam design with a SaniRay Atlantic germicidal low-

pressure lamp housed in a wooden box. The lamp sits in the top compartment of the box where light exposure can be controlled using a sliding wooden board through an open slot right below the lamp. The board can be removed to allow for irradiation of the sample or quickly reinserted to promptly stop exposure. The sample is housed in the bottom compartment of the wooden box on an adjustable prop below the opening of the lamp. The height of the prop can be re-adjusted depending on the desired time of UV exposure. The closer the sample is to the lamp, the faster the desired UV dose can be achieved. A stir plate is placed on top of the adjustable prop with the sample on top of the stir plate. The sample for this study was placed at a depth of 23.5-cm from the opening of the lamp to the sample surface in a cylindrical borosilicate glass crystallization (petri) dish. All exposed skin is covered when using the UV light system, along with UV blocking eye protection.

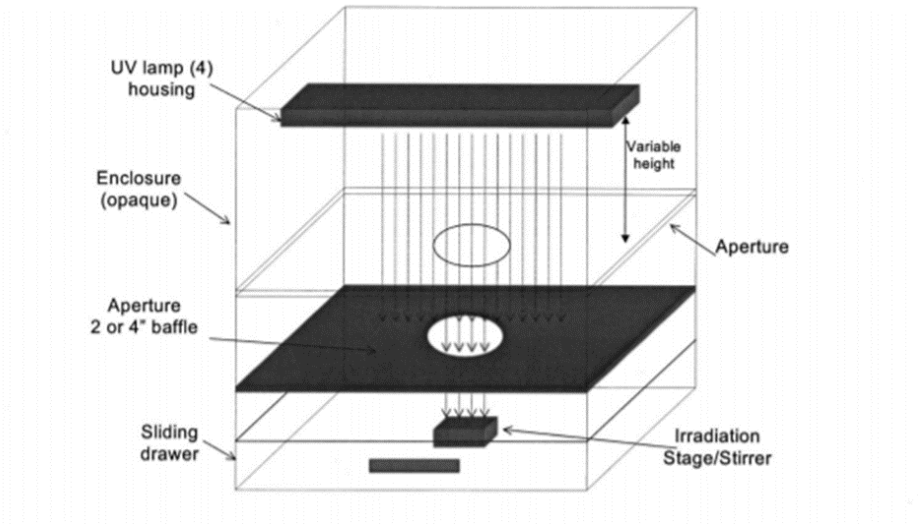

Figure 1: The UV system is based on the collimated beam design by Bolton and Linden, 2003

Figure 1 shows the collimated beam design from Bolton and Linden, (2003) and Figure 2 shows the adapted configuration used in this research.

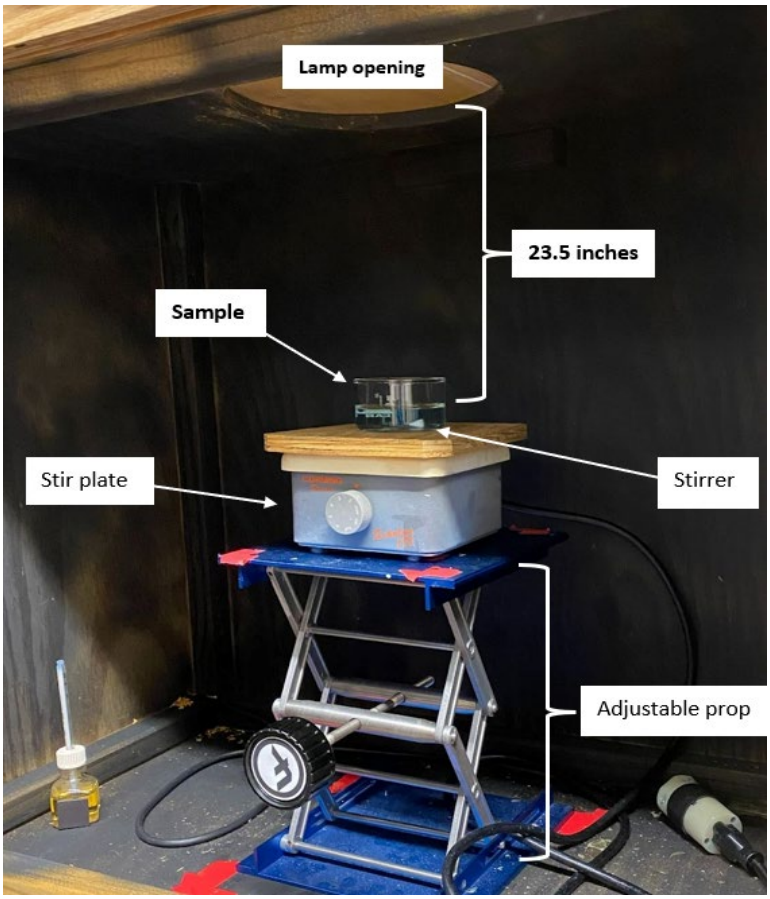

Figure 2: UV system configuration used for this research. The adjustable prop is used to obtain the consistent height of 23.5-inches between the water surface of the sample to the opening of the lamp. On top of the adjustable prop is a stir plate, a wooden prop to add additional height, and then the sample in a petri dish with a stirrer.

3.8 Absorbance Scan Methodology

A volume of 0.319 mL of stock solution methylene blue was added into both the headspace and no-headspace flasks that was previously prepared for the H_2O_2

measurements. Ensure the solution is homogenized by stirring adequately. With a clean 1-cm cuvette, add deionized water and allow the spectrophotometer to zero the absorbance between wavelengths 200 to 400-nm. After zeroing, add enough volume of the H_2O_2/Methylene Blue sample solution into a clean 1 cm cuvette and initiate the absorbance between wavelengths 200 to 400-nm. After a successful scan, data was transferred to excel for the following calculations to determine the appropriate time of exposure for each UV dose.

3.8.1 Absorbance Scan Calculations

The following calculations to determine the UV exposure time were adapted from Bolton and Linden, (2003). The exposure time for each UV dose is calculated based on certain parameters such as the measured lamp irradiance, the calculated petri factor (distribution of irradiance over the sample surface), the measured distance of the sample depth in the petri dish, and the distance between the UV lamp and the water surface of the sample within the petri dish. All calculations are based on wavelengths between 200 to 400-nm.

An International Light Technologies™ ILT2500 Flash Profiling Radiometer is used to measure the lamp irradiance in mW/cm^2. The irradiance measured by the radiometer will be the irradiance at the sample surface, therefore it is important that the radiometer sensor is placed exactly at the elevation the sample will be, which in this case is kept at 23.5 cm down from the opening of the UV lamp. The radiometer is first zeroed by keeping the cap over the sensor. After zeroing, the cap is removed, and the sensor is placed on the stir plate where the sample will be, and the highest reading is recorded.

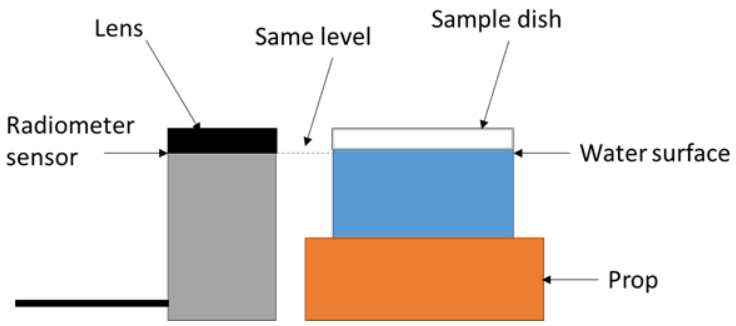

Figure 3: Configuration of the water sample surface relative to the radiometer sensor

The petri factor is a constant that accounts for uneven distribution of irradiance across the surface of the sample. It was calculated by taking the irradiance ($\mu W/cm^2$) in small 1-cm intervals along the x-axis and y-axis of the platform of which the sample will sit. The irradiance changes depending on the distance of the water surface of the sample for the lamp, therefore the Petri Factor was calculated based on a distance of 23.5 cm. The measurements were then normalized to set the highest reading to 1. The Petri Factor is calculated by taking the average of the normalized values across the surface of the 7-cm crystallization dish and dividing it by the highest value for a factor of 0.97 used in this experiment. This factor changes depending on the size of the petri dish. Generally, a factor of 0.90 is considered acceptable and the UV beam is considered to be adequately collimated.

For each headspace and no-headspace sample, 50-mL aliquots are distributed into three petri dishes. The sample depth in the petri dish was recorded as 1.6-cm, and should be no more than 1 to 2-cm. The distance from opening of the UV lamp to the water surface of the sample in the petri dish is kept at 23.5-cm.

The exposure duration for each dose of 100 mJ/cm^2 is then calculated based on the parameters described previously. Each sample is irradiated a total of 5 times for a total dose of 500 mJ/cm^2. The incident irradiance (mW/cm^2) is the incident light intensity delivered to liquid sample surface is calculated as:

$$\text{Incident Irradiance (mW/cm}^2\text{)} = \text{Radiometer reading (mW/cm}^2\text{)} \cdot (\text{Sensor Factor, } f_P) \cdot (\text{Petri Factor}) \cdot (\text{Reflection Factor}) \cdot (\text{Divergence Factor}) \quad (4)$$

where,

$$\text{Sensor Factor, } f_P = \Sigma \text{ RLE column} \div \Sigma\,[\text{RLE at wavelength } i \cdot f_R \text{ at wavelength } i)]. \quad (5)$$

The Relative Lamp Emission (RLE), also known as the Lamp Spectral Data, is normalized to equal 1 at wavelength 254 for low-pressure lamps or the sum of RLE to equal 1 for medium-pressure lamps, where i = specific wavelength between 200 to 400-nm, and f_R is calculated by the following equation,

$$f_R = R \div (R_{254}) \quad (6)$$

where R = Spectral Response Curve of Detector and R_{254} = R at 254 nm. The Reflection Factor is a unitless constant that accounts for when light passes from one medium to another, a fraction of beam is reflected off the interface, where R = fraction reflected. For

air and water, RF = 1 - R = 0.975. The Divergence Factor is a unitless constant that accounts for the divergence of the collimated beam and can be derived from the following equation:

$$\text{Divergence Factor} = \text{Sample Distance from Beam (cm)} \div [\text{Sample Distance from Beam (cm)} + \text{Sample Depth (cm)}] \quad (7)$$

where the divergence factor in this case is 0.935 as these distances remain constant through this research.

The Average Irradiance (mW/cm^2) is the average light intensity over the whole liquid sample volume, calculated from the following equations in sequential order. The first term, L_λ is the lamp energy output and can be calculated by taking the RLE and dividing by the sum of RLE as shown in equation 5:

$$L_\lambda = \text{RLE} \div (\Sigma\ \text{RLE}). \quad (8)$$

The Incident intensity per wavelength *i,* denoted as I_i, is calculated next as,

$$I_i = L_\lambda \cdot \text{Incident Irradiance } (mW/cm^2). \quad (9)$$

The average irradiance, l_{ave} is calculated next as the product of the incident intensity per wavelength *i* calculated from equation 9, and the Water Factor:

$$l_{ave} = I_i \cdot \text{Water Factor} \quad (10)$$

The Water Factor is determined by the following equation:

$$\text{Water Factor} = [1 - (10^{-[(Aw)(d)]})] \div [A_w \cdot d \cdot ln(10)] \quad (11)$$

where, A_w = water absorbance scan via Spectrophotometer over 200 to 300-nm wavelengths and d = sample depth (cm). Lastly, the final average irradiance (mW/cm^2) is equal to the sum of l_{ave} over 200 to 400-nm:

$$\text{Average Irradiance (mW/cm}^2\text{)} = \Sigma\, l_{ave} \quad (12)$$

The exposure time is the required time the sample in the petri dish is irradiated for every 100 mJ/cm^2 up to 500 mJ/cm^2, and can be calculated as:

$$\text{Exposure Time (sec)} = \text{UV Dose (mJ/cm}^2\text{)} \div \text{Average Irradiance (mW/cm}^2\text{)} \quad (13)$$

3.9 OH$^\bullet$ Scavenging Determination Methodology using Methylene Blue

The probe compound, methylene blue (MB) is used in this experiment to calculate the concentration of OH$^\bullet$ generated by assessing the decay of MB upon irradiation, which then will be incorporated into the calculation of the scavenging term. The following section summarizes the procedure to prepare the samples for irradiation.

Samples with H_2O_2 addition are distributed in 50-mL aliquots into three petri dishes for both headspace and no-headspace samples. Additionally, 50-mL aliquots of samples without H_2O_2 addition are distributed into three petri dishes. A single Teflon coated magnetic spin bar is added into each sample.

3.9.1 Dark Control

Dark controls are measured to ensure that concentrations of MB are kept constant with no UV light exposure and that decay of MB is due to irradiation and hydroxyl radical reaction. Approximately 10-mL of the sample is added to a 5-cm cuvette and the initial wavelength absorbance reading is measured at 664-nm and recorded. The 10-mL of sample is added back to the petri dish and placed in the UV box for the allotted time without UV light exposure. After the time is done, the sample is taken out of the UV box and 10-mL of the dark control sample is added to a 5-cm cuvette and the absorbance reading is measured at 664-nm and recorded. This process is repeated five more times to mimic every 100 mJ/cm^2 of UV dose the sample would receive during the irradiation process. There should be no decay measured from the initial reading for any of the readings.

3.9.2 Irradiation

For the irradiation process, the procedure is done exactly as the dark control except now with UV light exposure. An initial zero dose reading is measured and then the petri dish is placed in the UV light box for the exposure time required. After the exposure time, the exposure is promptly stopped, and the sample is removed from the UV box.

Approximately 10-mL of the irradiated sample is added to a 5-cm cuvette and the absorbance reading is measured at 664-nm and recorded. The 10-mL of sample is then added back to the petri dish to be irradiated again for a second dose. This procedure is repeated until the sample has received up to 500 mJ/cm^2. This process is then repeated for the remaining petri dishes and then repeated for samples without H_2O_2 addition. All measurements are recorded in an excel spreadsheet for processing described in the next section

3.10 Scavenging Term Methodology

The calculated measured $OH^{\bullet}$ scavenging is referred to as the scavenging term in this methodology, that is expressed as the summation of the products of their respective second order $OH^{\bullet}$ reaction rate constants, $k_{OH\bullet,\,S}$, and concentrations $[S_i]$:

$$\Sigma k_{OH\bullet,\,S_i} \cdot [S_i] = \Sigma k_{OH\bullet,1} \cdot [S_1] + \Sigma k_{OH\bullet,S_2} \cdot [S_2] + \Sigma k_{OH\bullet,S_3} \cdot [S_3] + \cdots \qquad (14)$$

The scavenging term is expressed as $\Sigma k[S]$ with a unit of measurements of s^{-1}. Water characteristics and composition vary from source to source, meaning $\Sigma k[S]$ is site specific. To optimize and understand the impact on AOP equipment, the magnitude of $\Sigma k[S]$ can be derived experimentally.

The scavenging term can be determined from Equation 15 by using the probe compound methylene blue and H_2O_2 to indirectly determine $\Sigma k[S]$. By mixing the probe compound and H_2O_2 into the sample water followed by irradiation, the degradation kinetics of the probe compound and the scavenging term can be determined with,

$$\Sigma k_{OH\bullet,S_i}[S_i] = \frac{ln(10) \cdot \epsilon_H \cdot \phi_H \cdot [H_2O_2] \cdot k_{OH\bullet,C}}{U_{254} \cdot k'_{OH\bullet}} \quad (15)$$

where,

$\epsilon_{H_2O_2}$ = the molar absorption coefficient of H_2O_2 (L $mol^{-1}cm^{-1}$);

ϕ_{OH} = the overall quantum yield for H_2O_2 photolysis at 254-nm (dimensionless);

$[H_2O_2]$ = the concentration of H_2O_2 in solution (mol/L);

$k_{OH\bullet,C}$ = the second order hydroxyl radical reaction rate constant of probe compound (L/mol/s);

U_{254} = the energy per mole of photons at 254 nm (J/mol);

$k'_{OH\bullet}$ = the experimentally obtained fluence based pseudo-first order rate constant for the probe (cm^2/mJ).

The following constants are used for equation 17: $\epsilon_{H_2O_2}$= 19 L $mol^{-1}cm^{-1}$ (Glaze et al., 1995), ϕ_{OH}= 1 (Glaze et al., 1995), $k_{OH\bullet,C}$ = 2.10 x 10^{10} L $mol^{-1}s^{-1}$ for methylene blue (Buxton et al., 1987), and U_{254}= 471,528 J/mol for radiation at 254 nm calculated based on the wavelength using Planck's equation. To determine $k'_{OH\bullet}$, the overall degradation rate k' observed for the probe compound is obtained from the following equation:

$$ln(A/A_O) = -k' \cdot F \quad (16)$$

where F is the fluence delivered to the sample volume (mJ/cm^2) that is obtained from the product of the exposure time (s) and the fluence rate (mJ/cm^2/s) as determined from the IUVA protocol (Bolton et al., 2015). The value of k' can be determined by linear

regression by plotting $ln(A/A_O)$ versus exposure time. Typically, both hydroxyl radical reaction and direct photolysis (although almost nonexistent for MB) will contribute to the degradation of the probe compound, therefore the value of $k'_{OH\bullet}$ can be obtained from the sum of the individual fluence based pseudo-first order rate constants as:

$$k' = k'_d + k'_{OH\bullet} \quad (17)$$

where k'_d is the direct photolysis rate constant and $k'_{OH\bullet}$ is the hydroxyl radical rate constant, both in units of cm^2/mJ. The value of k' can be obtained experimentally with the presence of H_2O_2 and k'_d can be obtained experimentally without the presence of H_2O_2, therefore $k'_{OH\bullet}$ can be calculated from the difference between the two: k' - k'_d.

3.11 Scavenging Term Correction

Once the scavenging term ($\Sigma k[S]$) is obtained, it must be corrected from the contributions of both the probe compound and H_2O_2. This is done by subtracting $\Sigma k[S]$ by the product of the second order rate constant and the concentration for each the probe compound and H_2O_2 using Equation 18, where [MB] is the molar concentration of the probe compound, methylene blue. The rate constant used for the probe compound, $k_{OH\bullet,C}$, is 2.10 x 10^{10} L/mol/s and the rate constant for hydrogen peroxide, $k_{OH\bullet,H_2O_2}$, 2.7 x 10^7 L/mol/s (Buxton et al., 1987).

$$\Sigma k[S] = \frac{ln(10) \cdot \epsilon_H \cdot \phi_H \cdot [H_2O_2] \cdot k_{OH\bullet,C}}{U_{254} \cdot k'_{OH\bullet}} - ([MB] \cdot k_{OH\bullet,C} - ([H_2O_2] \cdot k_{OH\bullet,H_2O_2}) \quad (18)$$

To derive the molar concentration of the probe compound, the Beer-Lambert law,

$$A = \varepsilon \times l \times C \quad (19)$$

was used to derive C by taking the average absorbance reading before irradiation of the H_2O_2 sample (UV dose 0), and dividing it by the product of the molar absorptivity (ε) and pathway length (l), where ε = 74,500 $M^{-1}cm^{-1}$ and l = 5-cm.

The theoretical scavenging (s^{-1}) consists of bicarbonate and DOC and can be calculated by summing the product of the second order rate constant and the concentration for each parameter, as shown in Equation 22. The rate constant for alkalinity is 8.50 x 10^6 L $mol^{-1}s^{-1}$ (Buxton et al., 1987) and for DOC is 3.6 x 10^8 L $mol^{-1}s^{-1}$ (Westeroff et al., 1998).

$$Theoretical\ Scavenging = ([HCO_3^-] \cdot k_{OH\bullet,HCO_3^-}) + ([DOC] \cdot k_{OH\bullet,DOC}) \quad (20)$$

The corrected scavenging term can be assessed for the DOC contribution by subtracting the product of the second order rate constant and the concentration of alkalinity and then dividing the value by the DOC concentration in mg-C/L to obtain the

effective second order OH• rate constant for the DOC (L mg-C^{-1} s^{-1}), described in Equation 21:

$$k_{OH\bullet,DOC} = \left[\frac{ln(10) \cdot \epsilon_H \cdot \phi_H \cdot [H_2O_2] \cdot k_{OH\bullet,C}}{U_{254} \cdot k'_{OH\bullet}} - \left([HCO_3^-] \cdot k_{OH\bullet,HCO_3^-}\right)\right] \div (DOC) \quad (21)$$

While contributions from the probe compound is present, it must be negligible enough in such that $\Sigma k[S]$ is kept constant. However, the initial concentration of the probe must be high enough to fully capture the degradation kinetics during the irradiation within a reasonable time. Therefore, the initial probe compound concentration must be higher than the limit of quantification, but its scavenging must be much lower than the value of $\Sigma k[S]$.

3.12 Uncertainty

3.12.1 Overall Observed Indirect Photolysis Rate Constant and Standard Error

The standard error of the indirect photolysis rate ($k' \pm \sigma_{H_2O_2}$) in units of s^{-1} is calculated by subtracting the average slope of the dark control from the average slope of the irradiated H_2O_2 sample to first determine k'. The standard error of the irradiated H_2O_2 (σ_{light}) sample is determined by taking standard error of the triplicate sets and summing the value obtained with the standard error of the three slope measurements of the dark control (σ_{dark}) with equation 22 to calculate the standard error:

$$\sigma_{H_2O_2} = (\sigma_{light}^2 + \sigma_{dark}^2)^{1/2} \quad (22)$$

3.12.2 Direct Photolysis Rate Constant and Standard Error

The standard error of the direct photolysis rate ($k'_d \pm \sigma_d$) in units of s^{-1} is calculated by subtracting the average slope of the dark control from the average slope of the irradiated sample with no H_2O_2 to first determine k'_d . The standard error of the irradiated sample with no H_2O_2 (σ_{light}) sample is determined by taking the standard error of the slope of the triplicate sets and summing the value obtained with the standard error of the three slope measurements of the dark control (σ_{dark}) with equation 23 to calculate the standard error:

$$\sigma_d = (\sigma_{light}^2 + \sigma_{dark}^2)^{1/2} \quad (23)$$

3.12.3 Indirect Photolysis Rate Constant and Standard Error

The standard error of the fluence based pseudo-first order rate constant ($k'_{OH\bullet} \pm \sigma_{OH\bullet}$) is calculated by summing the square of the standard error of the indirect and direct photolysis rate and then finding the square root:

$$\sigma_{OH\bullet} = (\sigma_{H_2O_2}^2 + \sigma^2{}_d)^{1/2} \quad (24)$$

3.12.4 Scavenging Term and Standard Error

The standard error of the measured scavenging value $\Sigma k[S]$ by using the calculated standard errors of the overall observed indirect photolysis rate ($\sigma_{H_2O_2}$), the fluence based pseudo-first order rate constant ($k'_{OH\bullet}$), and the associated standard error ($\sigma_{OH\bullet}$), and the concentration of H_2O_2 using the equation:

$$\sigma_{\Sigma k[S]} = \Sigma k[S] \cdot \{(\frac{\sigma_{OH\bullet}}{k'_{OH\bullet}})^2 + (\frac{\sigma_{H_2O_2}}{[H_2O_2]})^2 \quad (25)$$

3.13 Carbon Oxidation State Calculations

The average oxidation state of carbon atoms was calculated for each organic compound listed in Buxton et al., (1987), and tabulated with their respective reactivity rate with hydroxyl radicals. Oxidation states were calculated by analyzing Lewis structures and counting electrons, or following the methodology described in LaRowe et al., (2011) for compounds with standard elements containing carbon, hydrogen, nitrogen, oxygen, phosphorus, and sulfur from the following equation:

$$NOSC = -((-Z + 4a + b - 3c - 2d + 5e - 2f)/a + 4 \quad (26)$$

Where Z equals the net charge of the compounds, and $a, b, c, d, e,$ and f corresponds to the elements carbon, hydrogen, nitrogen, oxygen, phosphorus, and sulfur respectively (LaRowe et al., 2011).

Chapter 4: RESULTS AND DISCUSSION

4.1 Introduction

This chapter summarizes the results from the methodology described in the previous chapter followed by a review of the statistical significance. A thorough analysis between the average nominal carbon oxidation states (NOSC) of organic compounds and their respective reaction rate constants with hydroxyl radicals listed in Buxton et al., (1988) were evaluated first followed by an analysis of the experimental results. Experimental results were analyzed individually by season (summer and winter) and then compared between seasons for each site. Outliers and data gaps are evaluated and explained before applying statistical analysis. P-values were evaluated for various groups at a significance level of 0.05 using a t-Test. Correlations were analyzed by regression analysis and R^2 values.

4.2 Hydroxyl Radical Rate Constants as a Factor of Carbon Oxidation Number

Using the methodology described by LaRowe et al., (2011) for calculating the average nominal carbon oxidation states (NOSC) of organic compounds listed in Buxton et al. (1987), a t-Test was performed to determine if $OH^{\bullet}$ reaction rate constants were significantly higher for compounds with negative NOSC compared to positive NOSC. As mentioned in Chapter 1, it is hypothesized that reducing conditions of the water matrix will change the oxidation state of organic carbon atoms in NOM to be more reduced. Since reactions with $OH^{\bullet}$ are oxidation reactions, the radicals will have a greater affinity for these reduced organics and therefore scavenging rates will increase with decreasing

ORP of the water matrix. **Figure 4** shows the plotted results of each compound and the corresponding reactivity rates for over 1,000 organic compounds ($n = 1{,}003$).

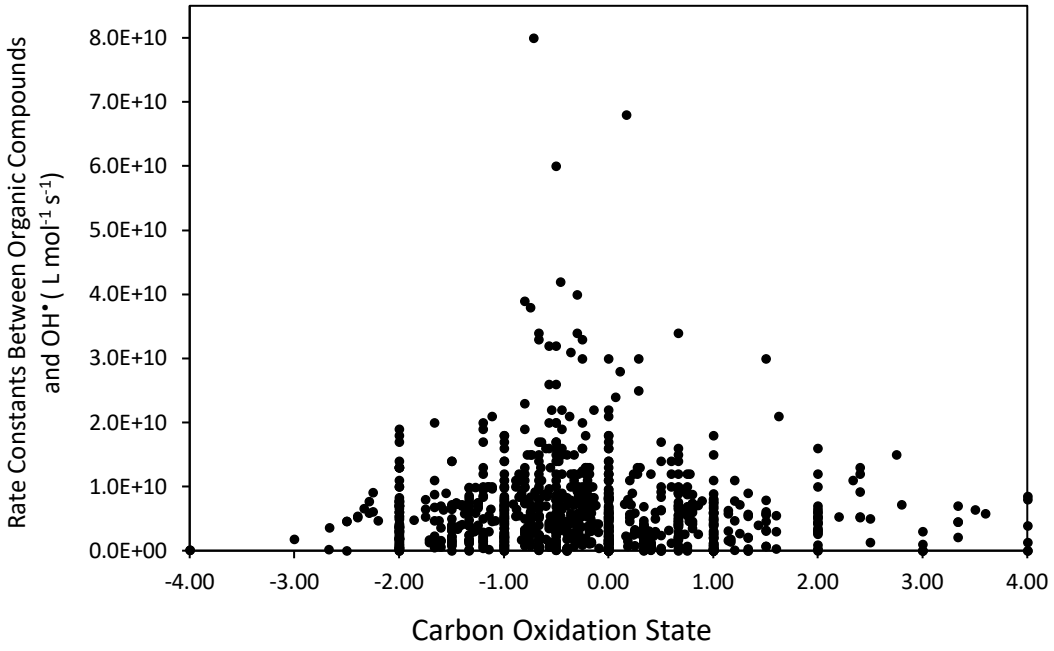

Figure 4: OH• second order reaction rate constants for organic compounds listed in Buxton et al., (1987) as a function of nominal carbon oxidation state.

Figure 4 summarizes the relationship between the NOSC for over 1,000 organic compounds and their respective second order reaction rate constants with hydroxyl radicals. Different subsets of data were evaluated for significance using a t-Test. The following table summarizes the p-value results for each relationship using a significance level of 0.05.

Table 2: Summary of P-values between NOSC and $OH^{\bullet}$ reaction rates, $\alpha = 0.05$

Analysis Group	Observations (n)	P-value
1. Negative NOSC / Zero NOSC	580 / 120	0.000818
2. Positive NOSC / Zero NOSC	303 / 120	0.737
3. Negative & Zero NOSC / Positive & Zero NOSC	700 / 423	0.000212
4. Negative & Zero / Positive NOSC	700 / 303	0.00167
5. Negative NOSC / Positive NOSC	580 / 303	0.000222
6. Negative NOSC / Zero & Positive NOSC	580 / 423	0.0000204

Based on these results, there is a very strong difference in hydroxyl radical reaction rate constants with organic compounds based on the NOSC. This finding would suggest that the overall oxidation state of carbon in organic compounds is likely a driving factor or contributor behind how fast a reaction occurs with hydroxyl radicals and indicates that the net extra electrons on the carbons are attractive targets for $OH^{\bullet}$ radicals. As a result, this would support our first hypothesis that the oxidation state of carbon can influence how fast the reaction with hydroxyl radicals occurs. The average mean rate constant with $OH^{\bullet}$ with carbon with negative NOSC is 7.0×10^9 L mol^{-1} s^{-1}, with zero NOSC is 5.1×10^9 L mol^{-1} s^{-1}, and with positive NOSC is 5.2×10^9 L mol^{-1} s^{-1}. Higher rate constants are seen in relatively more reduced states of carbon (negative NOSC) compared to rate constants with compounds of higher NOSC.

This significance is critical in further investigating the driving factors behind $OH^{\bullet}$ scavenging by NOM in the experimental portion of this study. By changing the environmental redox conditions of the water matrix, the change in oxidation state of organic matter (and thus carbon) may influence hydroxyl radical scavenging. It was

observed in humic substances that redox-active moieties can behave as redox-buffers by becoming electron acceptors under anoxic conditions and electron donors under aerobic conditions **(Aeschbacher et al., 2009)**. By storing samples for analysis of scavenging term with headspace and no headspace in amber glass bottles, the changing redox conditions of the sample matrix could lead to differences in hydroxyl radical scavenging by DOC and total scavenging as a result, as DOC is the most influential contributor to overall scavenging term in most matrices.

4.3 Experimental Data Sets

Table 3 summarizes the pertinent data for each water source separated by the season during which the samples were obtained and when the experiments occurred. Winter samples were obtained and analyzed from January to February 2022 and summer samples were obtained and analyzed July to August 2022. The measured $OH^{\bullet}$ scavenging, the calculated DOC second order rate constant, ORP, and DOC concentration is listed for each sample at various hold times. Appendix A contains the comprehensive raw data collected from every sample that includes pH values, alkalinity, temperature, irradiance, absorbance scans, probe compound absorbance readings, and the probe compound concentration at UV dose of 0 mJ/cm^2 (initial dose).

Table 3: Results for Concord - $OH^{\bullet}$ scavenging, DOC rate constants, ORP, and DOC concentrations

Concord	Hold Time	Avg. $OH^{\bullet}$ Scavenging (s^{-1})	Avg. DOC Rate Constant (L mg-$C^{-1}s^{-1}$)	ORP (mV)	Avg. DOC (mg-C/L)
Winter Initial	0 HR	1.2×10^5	1.8×10^4	353	1.89
Winter HS	24 HR	1.9×10^5	3.3×10^4	238	1.94
	72 HR	8.0×10^4	9.4×10^3	245	2.01
Winter No HS	24 HR	1.1×10^5	1.7×10^4	224	1.87
	72 HR	7.3×10^4	7.7×10^3	214	1.86
Summer Initial	0 HR	9.4×10^4	1.6×10^4	140	1.6
Summer HS	24 HR	8.5×10^4	1.4×10^4	174	1.48
	48 HR	7.7×10^4	1.3×10^4	185	1.52
	72 HR	6.8×10^4	9.2×10^3	235	1.52
	7 DAYS	6.8×10^4	9.1×10^3	251	1.51
	14 DAYS	8.5×10^4	1.4×10^4	223	1.5
Summer No HS	24 HR	7.5×10^4	1.1×10^4	168	1.57
	48 HR	8.0×10^4	1.3×10^4	181	1.58
	72 HR	6.9×10^4	9.4×10^3	224	1.55
	7 DAYS	7.4×10^4	9.1×10^3	249	1.53
	14 DAYS	8.9×10^4	1.5×10^4	224	1.55

Table 4: Results for Mount Holly - $OH^{\bullet}$ scavenging, DOC rate constants, ORP, and DOC concentrations

Mount Holly	Hold Time	Avg. $OH^{\bullet}$ Scavenging (s^{-1})	Avg. DOC Rate Constant (L mg-$C^{-1}s^{-1}$)	ORP (mV)	Avg. DOC (mg-C/L)
Winter Initial	0 HR	1.0×10^5	9.1×10^4	--	1.13
Winter HS	24 HR	8.3×10^4	7.5×10^4	273	1.08
	48 HR	8.5×10^4	4.3×10^4	305	1.38
	72 HR	8.3×10^4	7.2×10^4	168	1.15
	7 DAYS	5.8×10^4	4.9×10^4	141	1.05
Winter No HS	24 HR	8.3×10^4	7.5×10^4	282	1.91
	48 HR	1.1×10^5	7.8×10^4	283	1.12
	72 HR	6.5×10^4	5.4×10^4	177	1.13
	7 DAYS	6.4×10^4	6.0×10^4	158	1.08
Summer Initial	0 HR	8.0×10^4	7.5×10^4	265	1.05
Summer HS	*24 HR	3.2×10^5	3.6×10^5	287	0.88
	48 HR	6.0×10^4	8.6×10^4	251	0.67
	72 HR	5.6×10^4	4.2×10^4	264	1.27
	7 DAYS	7.4×10^4	6.0×10^4	210	1.19
	14 DAYS	5.4×10^4	4.5×10^4	203	1.15
Summer No HS	24 HR	6.5×10^4	5.6×10^4	282	1.12
	*48 HR	2.9×10^5	2.5×10^5	242	1.12
	72 HR	5.2×10^4	4.9×10^4	255	1.01
	7 DAYS	5.8×10^4	6.0×10^4	212	1.11
	14 DAYS	4.9×10^4	4.3×10^4	200	1.10

*Outliers due to scavenging values much higher than expected compared to the range of values from the other samples, which is further discussion in Section 4.5.

4.4 Missing Data

Due to the nature of this research requiring specific hold times, some data points are missing from unexpected events. For Concord Winter samples in Table 3, data points were not collected at hold times of 48 HR due to the closure of the University during an ice storm on January 21, 2022. Data collection was discontinued after 72 HR due to the

instability of the $OH^{\bullet}$ scavenging term. All data points were collected from hold times of 0 HR to 14 days as planned during the summer sampling period for Concord.

For Mount Holly Winter samples summarized in Table 4, the 0 HR data was collected, however it was excluded due to unexpected troubleshooting the ORP and pH meter that resulted in inconsistencies and unrepresentativeness of the data. However, ORP and pH do not directly contribute to the scavenging calculations therefore the measured scavenging and DOC rate constants are still used for interpretation where ORP and pH are not required for analysis. Data collection was discontinued after the 7 Day hold time due to the instability of the $OH^{\bullet}$ scavenging term. All data points were collected from hold times of 0 HR to 14 days as planned during the summer sampling period for Mount Holly.

4.5 Outliers

All measured hydroxyl radical scavenging datasets were analyzed for outliers that could potentially skew the results. Data sets were divided by source and season, and outliers were identified using two methods: Box Plot and the Interquartile Range (IQR).

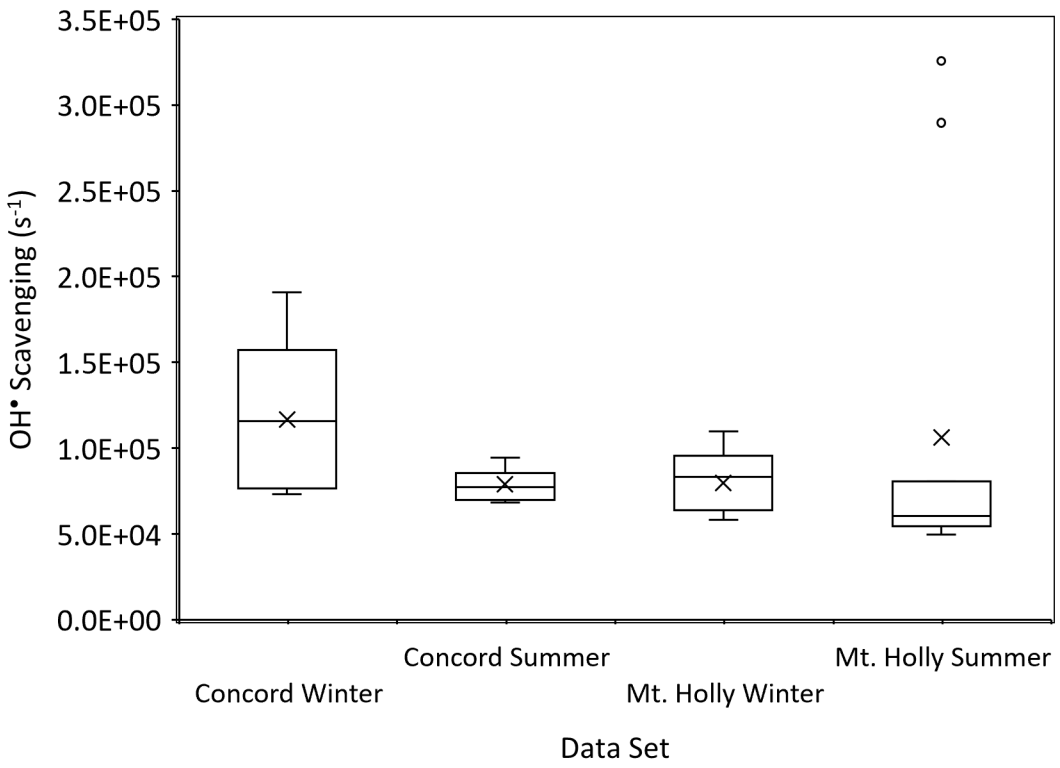

Figure 5: Distribution of data sets and outliers identified for the measured OH• scavenging term

Figure 5 shows a box plot of all data sets sorted by source and season to understand the data distribution and to identify outliers. Based on this chart there are a total of two outliers in the Mount Holly Summer data set. The next method using the IQR is summarized below in Table 5 to identify outliers that might not have shown on the box plot.

Table 5: Outliers by IQR

Outliers	Concord Winter	Concord Summer	Mt. Holly Winter	Mt. Holly Summer
Q1	8.0×10^4	7.2×10^4	6.4×10^4	5.5×10^4
Q3	1.2×10^5	8.5×10^4	8.5×10^4	7.7×10^4
IQR	4.3×10^4	1.3×10^4	2.0×10^4	2.2×10^4
Lower Limit	1.4×10^4	5.2×10^4	3.3×10^4	2.2×10^4
Upper Limit	1.8×10^5	1.1×10^5	1.1×10^5	1.1×10^5

Based on the upper and lower limits of each data set, the same two outliers identified in the box plot were also identified using the IQR. One outlier has a measured scavenging term of 3.2×10^5 s^{-1} for the 24 HR headspace and the second outlier has a measured scavenging term of 2.9×10^5 s^{-1} for the 48 HR no headspace sample, both above the upper limit defined by the IQR analysis.

For the outliers, absorbance measurements reveal slower than normal decay of the probe compound during irradiation of the sample with hydrogen peroxide, meaning $OH^{\bullet}$ radicals are being scavenged at a much higher rate which suggests a presence of additional scavenging compounds. Irradiance is intermittently checked several times throughout each experiment, and the radiometer readings were stable, which ruled out a possible equipment error associated with the lamp. The spectrophotometer passed all calibration checks and absorbance scans were successfully zeroed before taking dark control absorbance readings that were stable before the irradiation. Based on this, possible equipment error associated with the spectrophotometer was unlikely. Possible equipment and experimental errors were unlikely since the readings were as expected for the 24 HR no headspace sample and for the 48 HR headspace sample. However, the

presence of an unknown compound was detected on the absorbance scan for the two Mount Holly outliers as shown in Figure 6.

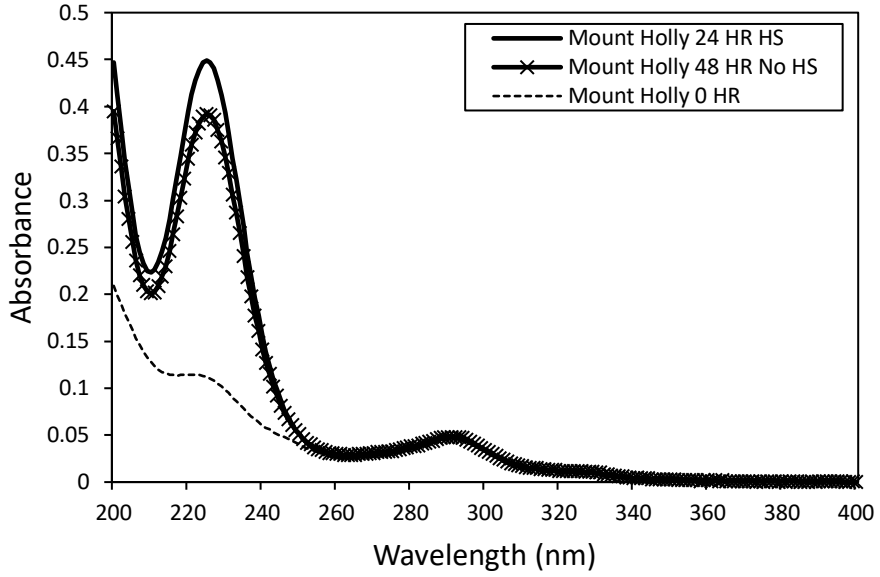

Figure 6: Absorbance Spectrum of the Mount Holly outlier samples with an unknown compound present compared to an absorbance spectrum for the initial day sample.

4.5.1 Potential Interference from Bisulfides (HS^-)

Based on the absorbance spectrum for both the Mount Holly outliers in Figure 6, the likely source of minimal decay of MB and high scavenging of $OH^{\bullet}$ was potentially due to the presence of an inorganic substance. When comparing the absorbance spectrum of the Mount Holly 0 HR sample to the outlier samples, the spectrum for the DOC concentration (first peak at 292-nm) were all the same as expected, however the second peak at 225-nm for the outlier samples is prominent compared to the 0 HR sample, indicated that the unknown substance originally had very little absorbance and converted

to something with a stronger absorbance while in storage. DOC remained relatively constant in those samples (0.88 mg/l for 24 HR HS and 1.12 mg/l for 48 HR no HS.

Due to the addition of aluminum sulfate during water treatment, it was originally thought that sulfate could have been reduced to hydrogen sulfide species through anaerobic microbial processes (Xu et al., 2013) in storage. Based on the sample pH measured on testing day of approximately 7.5, it was likely more dominated by HS^- species based on the pK_A values for H_2S which are $pK_{A1} = 7.1$ and $pK_{A2} = 14$ (Snoeyink and Jenkins, 1980).

To confirm whether the new absorbance peak in the two Mount Holly samples were caused by bisulfides, a stock solution using sodium hydrosulfide hydrate flakes dissolved in ultrapure water was prepared. With a 1-cm quartz cuvette and using the HACH DR6000 Spectrophotometer, the absorbance spectrum for HS^- concentrations of 3.0 mg/L, 5.0 mg/L, and 7.0 mg/L were then obtained and plotted in Figure 7. Additionally, the absorbance spectrum for the one of the outlier spectrums (Mt. Holly 48 HR No HS) was also plotted for comparison.

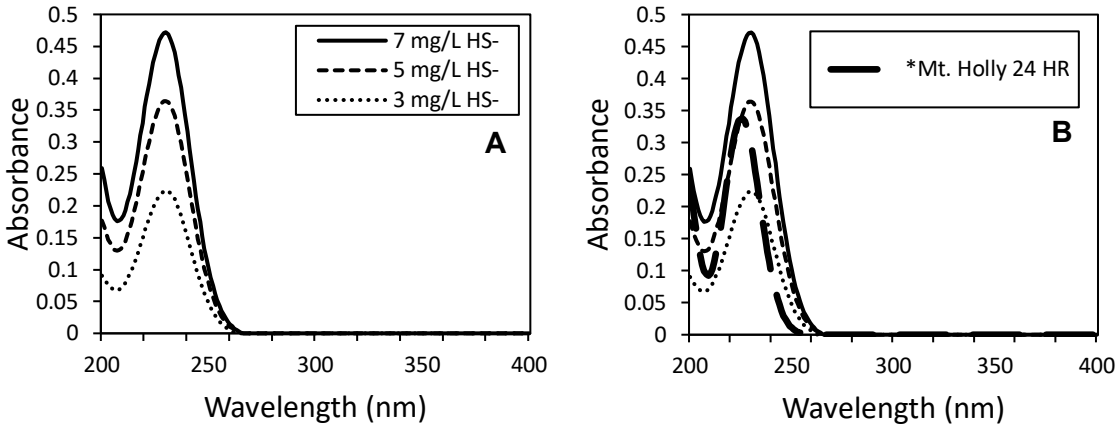

Figure 7: Absorbance spectrum at various concentrations of HS^- (A) and absorbance of Mt. Holly 24 HR No HS spectrum (thickest dashed lines) for comparison (B).

The Mount Holly outlier spectrum follows similar peaks and trends as the HS^- scans, however the peak for the HS^- is at 230 nm while the peak for the Mount Holly outliers is at 225 nm. To rule out potential influence of background constituents in the Mount Holly samples that could have shifted the peak by 5-nm, non-outlier Mount Holly samples were spiked with 3 mg/l, 5 mg/l, and 7 mg/l HS^- to compare the spectrums.

Figure 8 shows the corrected absorbance spectrum of the 7 mg/l spiked sample to compare with the 7 mg/l HS^- solution. The spiked absorbance scan was corrected by subtracting the initial day sample absorbance scan.

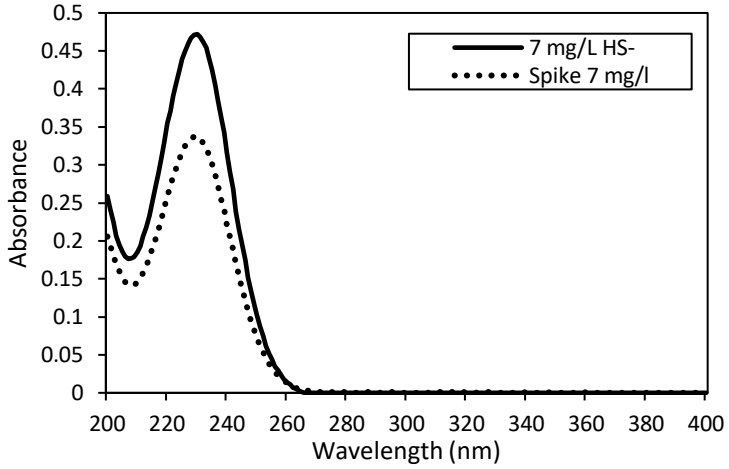

Figure 8: Absorbance spectrum of HS^- and spiked Mount Holly samples. HS^- absorbance spectrums in shown in dashed lines and the corrected spike samples in solid lines

The spiked sample shows the same peak at 230-nm as the pure bisulfide absorbance spectrum and not the same peak at 225-nm as seen in the outlier samples. Due to this difference, the unknown compound present is not likely bisulfides but could be structurally similar. The average molar absorptivity was calculated using the absorbance spectrum for HS^- concentrations at 3 mg/L, 5 mg/L, and 7 mg/L using a pathlength of 1-cm. Overall, this bisulfide study provides helpful data to identify the presence of this compound in water samples, especially for groundwater.

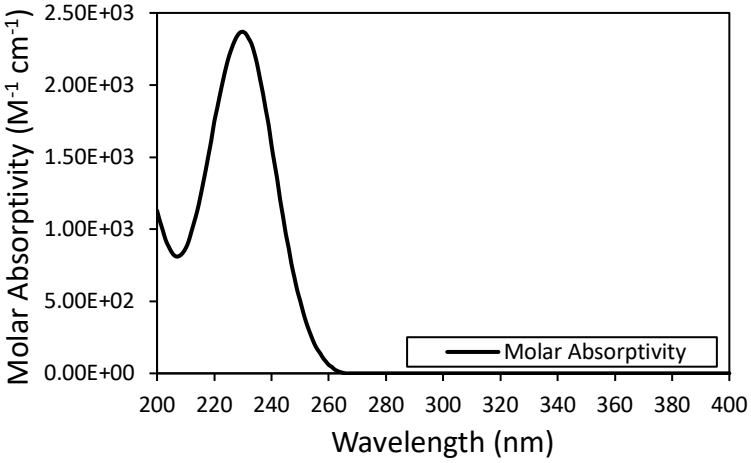

Figure 9: Average Molar Absorptivity (ε) for HS^- spectrum using a pathlength of 1-cm

Based on the bisulfide study, it was likely the Mount Holly outliers were contaminated with an unknown inorganic compound and excluded from the data set for statistical analysis to avoid unrepresentative skewness of the results. Figure 10 shows the new distribution of each data set that excludes outliers for the Mount Holly Summer samples except for the Concord Summer outlier.

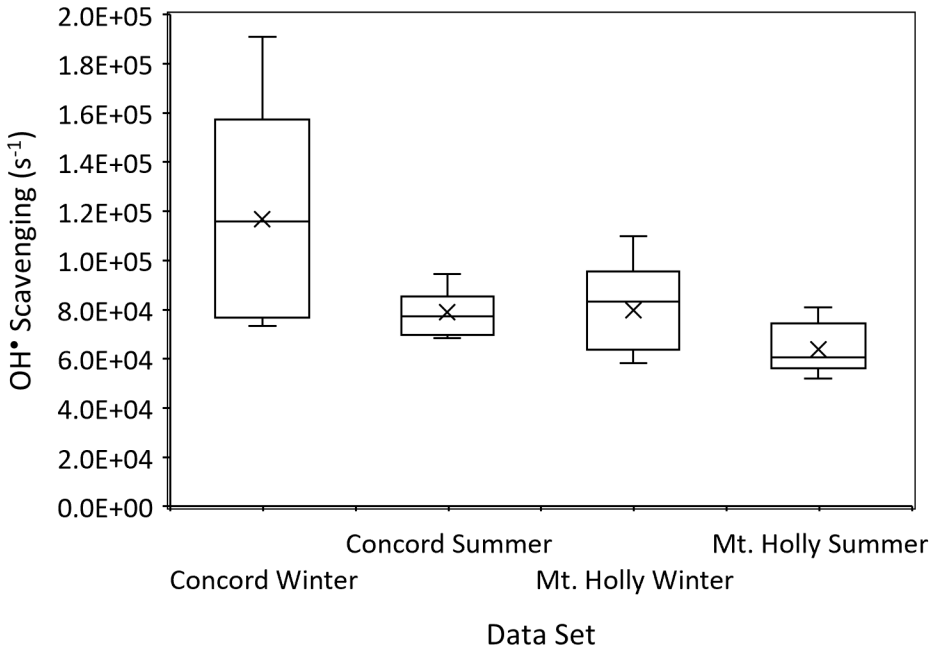

Figure 10: Distribution of data sets without outliers for the measured OH• scavenging term

4.5.2 Potassium Permanganate ($KMnO_4$) Quenching of H_2O_2

The Concord water treatment plant implements a pretreatment process of their raw influent by the addition of potassium permanganate to oxidize iron and manganese present. While it is important to obtain samples with no chlorine present, the potential interactions of OH• treatment with potassium permanganate remains largely unknown. Because the chemical is added in the pretreatment process, a residual is unlikely by the time the samples were obtained further downstream after filtration.

To understand the potential effects of residual potassium permanganate in this study, a stock solution was made with potassium permanganate powder dissolved in ultra-pure water. 1.0 mg/L $KMnO_4$ was first added to 160 mL of ultrapure water and mixed, followed by the addition of approximately 5 mg/L of H_2O_2 where the time of

addition is noted. The concentration of the H_2O_2 was then measured three times to assess whether concentration decreases. The same procedure was done with 3.0 mg/L $KMnO_4$ as well. A blank sample with only H_2O_2 with no $KMnO_4$ added was also measured for comparison. Table 6 summarizes the results below:

Table 6: Potassium Permanganate / H_2O_2 Quenching Study

Trial No. 1: 3.0 mg/L $KMnO_4$			Trial No. 2: 1.0 mg/L $KMnO_4$		
Time of H_2O_2 Measurement	H_2O_2 Concentration Measured (mg/l)	H_2O_2 Blank (mg/l)	Time of H_2O_2 Measurement	H_2O_2 Concentration Measured (mg/l)	H_2O_2 Blank (mg/l)
12:30, H_2O_2 Added			12:57, H_2O_2 Added		
12:41	5.40	5.56	13:01	5.05	5.46
12:46	5.44	5.11	*13:05	4.94	5.18
*12:52	4.21	5.31	13:07	4.53	5.27

*Measurement taken after notable color change of the solution from pink to pale orange to clear

In Table 6, the first column under each trial records the time stamp of when the concentration of H_2O_2 was measured relative to the time when H_2O_2 was added to the solution. The second column summarizes the H_2O_2 concentration with $KMnO_4$ present and the third column records the H_2O_2 concentration without $KMnO_4$.

During the experiment, the pink color of the solution contributed by $KMnO_4$ noticeably changed to a pale orange before turning clear after the addition of H_2O_2. This is due to hydrogen peroxide reducing $KMnO_4$ to Mn^{2+}, which is colorless through the following reaction (Bailey and Taylor, 1937):

$$2MnO_4^-(aq) + 5H_2O_2(aq) + 6H^+ \rightarrow 8H_2O(l) + 5O^2 + 2Mn^{2+}(aq) \quad (27)$$

The asterisk within the table designates the measurement of H_2O_2 after this change was observed. Under Trial No. 1, the first two measurements were stable until the color change where H_2O_2 concentration sharply declined. Under the second trial, the color change occurred faster after the addition of H_2O_2, where the third measurement shows a sharp decrease compared to the first two measurement. This implies that there is potentially an interference if a residual concentration of $KMnO_4$ was present in the water samples however, based on reaction 27, 0.7 mg/l of H_2O_2 would react with 1 mg/l of MnO_4, meaning a small residual would not drop the concentration of H_2O_2 by much. Concentrations of H_2O_2 were lower during the summer sampling event, reporting between 3 – 5 mg/l compared to winter concentrations of 4 – 6 mg/l, despite using the same volume consistently. However, it is more likely due to the stock solution of H_2O_2 degrading overtime rather than the presence of $KMnO_4$. A residual is unlikely after the oxidation of iron and manganese during the pretreatment process, as well as after coagulation/flocculation, sedimentation, and filtration.

4.5.3 Potassium Permanganate UV Irradiation Study

To study effects of $KMnO_4$ on MB under UV irradiation, a new solution of 160 mL ultra-pure water, 0.1 mg/L of $KMnO_4$ and 500 µM of MB was prepared. Using the same methodology described in Chapter 3, each petri dish of the $KMnO_4$/MB solution was exposed to UV light for a total fluence of 500 mJ/cm^2. The decay of MB was minimal as shown in Figure 11A. The presence of $KMnO_4$ can be visually detected at concentrations as low as 0.05 mg/l (Backer, 2017), therefore any residual $KMnO_4$ in the

Concord samples would be less than this concentration as there were no visual pink coloration in the samples and would be unlikely to interfere with the analysis. A blank was also measured with only MB and no $KMnO_4$ to compare the decay of MB and summarized in Figure 11. Additionally, Figure 11 (A) plots the normalized absorbance readings of MB for each experiment, with Figure 11 (B) showing the absorbance spectrum of $KMnO_4$. Based on the absorbance spectrum, photoactivity is unlikely because of very low absorbance at 254 nm, which is the wavelength emitted by the lamp.

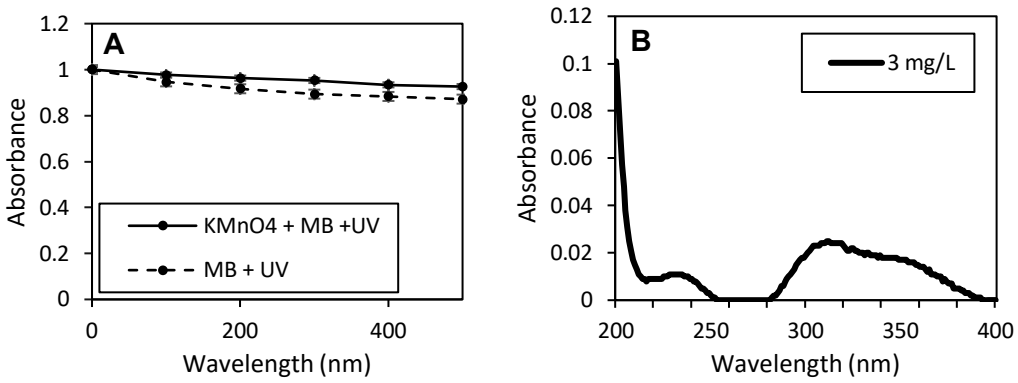

Figure 11: Comparing the decay of MB with and without $KMnO_4$ with standard error bars based on triplicate measurements (A) and Absorbance Spectrum of KMnO4 (B)

4.6 Analysis of ORP Changes

In theory, samples stored with oxygen present can readily become more oxidized overtime while in storage from the available oxygen, and samples stored with no headspace can become more reduced with no oxygen present. To rule out potential ORP changes due to the addition of H_2O_2 that might interfere with the scavenging process during UV irradiation, ORP measurements were taken before and after the addition of 5.0

mg/l of H_2O_2 for several Concord and Mount Holly water samples. Table 9 summarizes the findings.

Table 7: ORP Changes Before and After H_2O_2 Addition

ORP Before (mV)	ORP After (mV)
196	199
193	214
203	227

ORP very slightly increased after the addition of H_2O_2, but the changes are not significantly different (p-value: 0.134, $\alpha = 0.05$) and unlikely to interfere with the analysis of correlation between ORP and scavenging.

4.6.1 ORP Changes in Storage

To assess whether storage conditions were enough to allow ORP to naturally drift apart from the initial day, a t-Test was used for significant differences between the two conditions. The average ORP measurements and p-values between HS and no HS samples are summarized in Table 10.

Table 8: P-values for ORP measurements between HS and no HS, $\alpha = 0.05$

Data Set	HS ORP Average (mV)	No HS ORP Average (mV)	P-value
Concord Winter	241	219	0.066
Concord Summer	213	209	0.84
Mount Holly Winter	221	225	0.952
Mount Holly Summer	232	237	0.836

All p-values are non-significant, with Concord samples showing higher averages for the HS sample compared to without HS, but the differences between the datasets were not strong enough to draw significant conclusions that storage methods are impacting the redox conditions. Concord ORP values ranged from a minimum of 140 mV, a maximum of 353 mV, and an average of 221 mV. Mount Holly ORP values ranged from a minimum of 140 mV, a maximum of 305 mV, and an average of 217 mV.

4.7 Analysis of $OH^{\bullet}$ Scavenging

4.7.1 Temperature Experiments

Samples on collection day were at room temperature during the time of analysis compared to the subsequent samples tested at hold times after the initial day. Due to this an experiment was carried out on samples at two distinct temperatures of 9˚C and 20.3˚C to analyze the potential differences due to temperature. Table 11 summarizes the results below.

Table 9: Summary of Results for Temperature Experiment

Parameter	Sample 1	Sample 2
Temperature (°C)	9	20.3
pH (s.u.)	7.02	6.9
ORP (mV)	228	226
Avg. DOC (mg-C/l)	0.2555	0.2438
Bicarbonate Alkalinity (mol/L)	0.00052	0.000518
Avg. OH Scavenging (s^{-1})	6.4×10^4 +/- 2.8×10^3	5.1×10^4 +/- 4.6×10^3
Avg. DOC Rate Constant (L mg-$C^{-1}s^{-1}$)	2.3×10^4 +/- 1.2×10^5	1.9×10^4 +/- 1.9×10^4

Based on the results for both distinct temperatures, results for all parameters were slightly lower for the room temperature sample (20.3°C) compared to the cold sample (9°C). P-value results ($\alpha = 0.05$) for scavenging and DOC rate constants between the two samples is 0.039 and 0.057 respectively, drawing the conclusion that scavenging between the two samples at different temperatures are significantly different and that samples should be maintained at consistent temperatures.

4.7.2 $OH^{\bullet}$ Scavenging of Samples

The following sections analyze differences in $OH^{\bullet}$ scavenging under HS and No HS storage conditions and significant drifting in scavenging from the initial day. Table 11 and Table 12 summarizes the p-value results of scavenging differences based on storage conditions.

Table 10: P-values for $OH^{\bullet}$ Scavenging between Concord HS and no HS, $\alpha = 0.05$

	Data Set	P-value
Concord Winter	24 HS	0.026
	24 No HS	
	72 HS	0.011
	72 No HS	
Concord Summer	24 HS	0.066
	24 No HS	
	48 HS	0.325
	48 No HS	
	72 HS	0.166
	72 No HS	
	7 DAY HS	0.305
	7 DAY No HS	
	14 DAY HS	0.553
	14 DAY No HS	

Only Concord Winter scavenging values were significantly different between HS and no HS storage conditions. As for Concord Summer, no scavenging differences between HS and No HS were significant.

Table 11: P-values for $OH^{\bullet}$ Scavenging between Mt. Holly HS and no HS, $\alpha = 0.05$

Data Set		P-value
Mt. Holly Winter	24 HS	0.422
	24 No HS	
	48 HS	0.0454
	48 No HS	
	72 HS	0.0424
	72 No HS	
	7 DAY HS	0.326
	7 DAY No HS	
Mt. Holly Summer	24 HS	0.0019
	24 No HS	
	48 HS	0.0064
	48 No Hs	
	72 HS	0.116
	72 No HS	
	7 DAY HS	0.167
	7 DAY No HS	
	14 DAY HS	0.0207
	14 DAY No HS	

Mount Holly Winter samples did not reveal differences in scavenging between storage conditions until 48 HR hold times but then leveled out by day 7. Mount Holly Summer scavenging was significantly different within the 24 HR, 48 HR, and 14 Day hold times only. Based on these results, the testing of $OH^{\bullet}$ scavenging in AOPs should consider storage conditions as values can differ significantly with HS and no HS present. While ORP changes were not strong between the storage conditions, other factors such as DOC composition and concentration could contribute to these differences throughout the seasons.

Table 13 summarizes significant differences in $OH^{\bullet}$ scavenging at various hold times compared to the initial day.

Table 12: $OH^{\bullet}$ Scavenging Hold Time Changes from Initial Day, $\alpha = 0.05$

Sample	Hold Time	Headspace	No Headspace
		P-value	
Winter Concord	24 HR	0.012	0.448
	72 HR	0.038	0.027
Summer Concord	24 HR	0.105	0.0002
	48 HR	0.014	0.103
	72 HR	0.004	0.006
	7 DAY	0.052	0.173
	14 DAY	0.068	0.513
Winter Mt. Holly	24 HR	0.002	0.021
	48 HR	0.097	0.016
	72 HR	0.0003	0.0002
	7 DAY	0.023	0.0006
Summer Mt. Holly	24 HR	0.003	0.125
	48 HR	0.001	0.014
	72 HR	0.043	0.009
	7 DAY	0.080	0.106
	14 DAY	0.001	0.00005

52% of the results were significant for both HS and no HS, drawing the conclusion that there is significant drifting in scavenging from sampling day and therefore making it important to test for scavenging within 24 HR to accurately assess the magnitude of $OH^{\bullet}$ scavenging before results can become erroneous despite storage conditions. Five analyses were non-significant for samples stored with HS while six were within the no HS condition, meaning drifting is consistent regardless of storage conditions. Oxygen present could allow for reactions to occur within the sample during storage, and subsequently change scavenging at a greater magnitude compared to the initial day.

Based on results in Table 11, 12, and 13, testing of OH• scavenging in AOPs should consider storage conditions and hold times as both analyses revealed significant drifting of scavenging under both storage conditions and at different hold times.

4.7.4 ORP and OH• Scavenging Trends at Different Hold Times

Figure 12 plots the measured OH• scavenging and ORP values for headspace and no headspace at various hold times with standard error bars calculated using the methodology described in section 3.12.

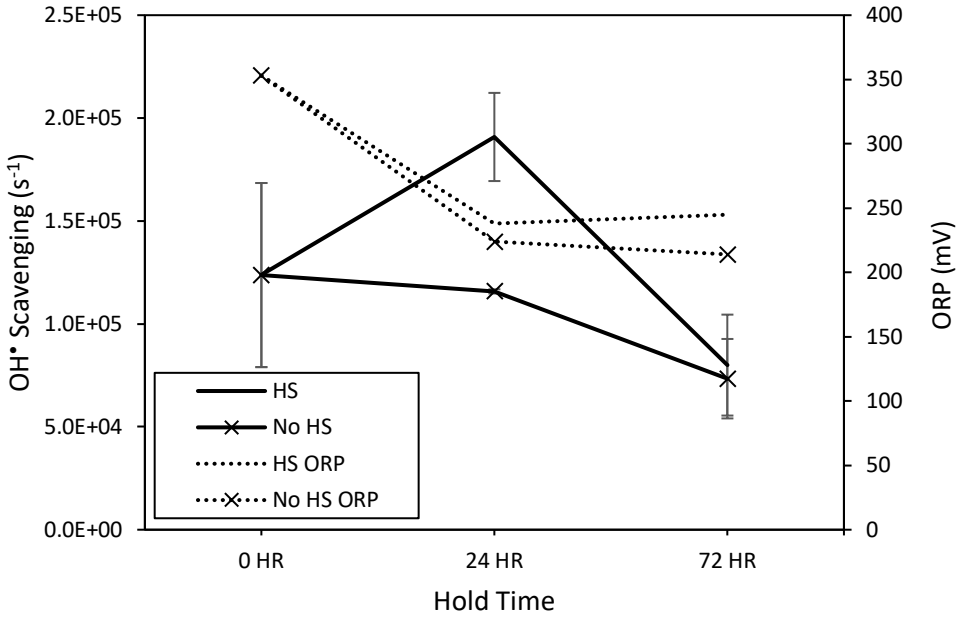

Figure 12: OH• Scavenging (solid lines) and ORP trends (dashed lines) for Winter Concord samples over time

In Figure 13, the ORP and HS scavenging reveal negative correlations over time while no HS scavenging steadily decreases as ORP continues to decrease as well. Although storage conditions resulted in no significant differences in ORP, the scavenging remained consistently lower for samples under no HS conditions compared to HS.

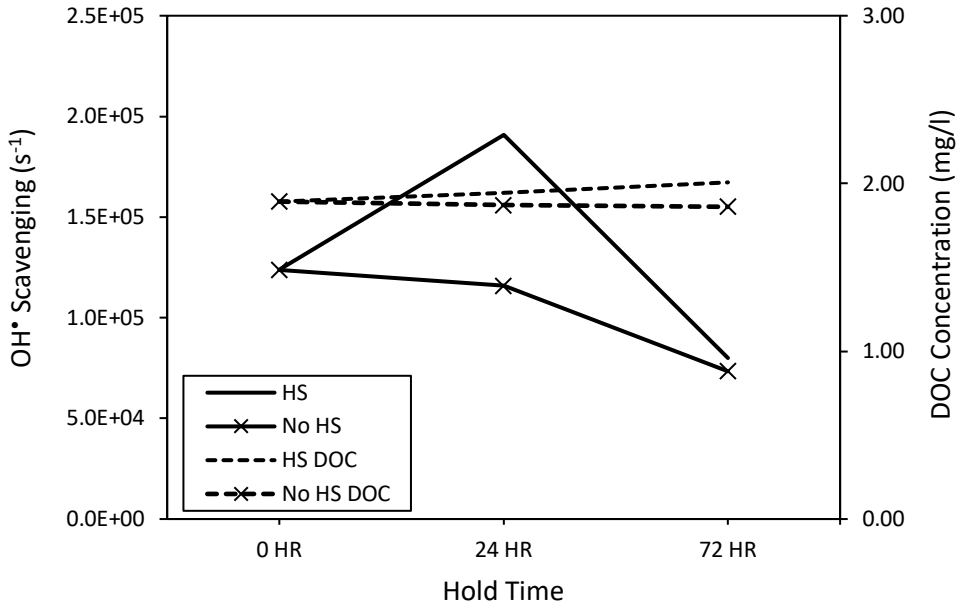

Figure 13: OH• Scavenging and DOC trends for Winter Concord samples over time

When comparing scavenging to DOC concentrations in Figure 14, HS DOC and no HS DOC remained relatively constant. Concentrations reached a maximum of 2.01 mg-C/l and a minimum of 1.86 mg-C/l between both HS and no HS samples.

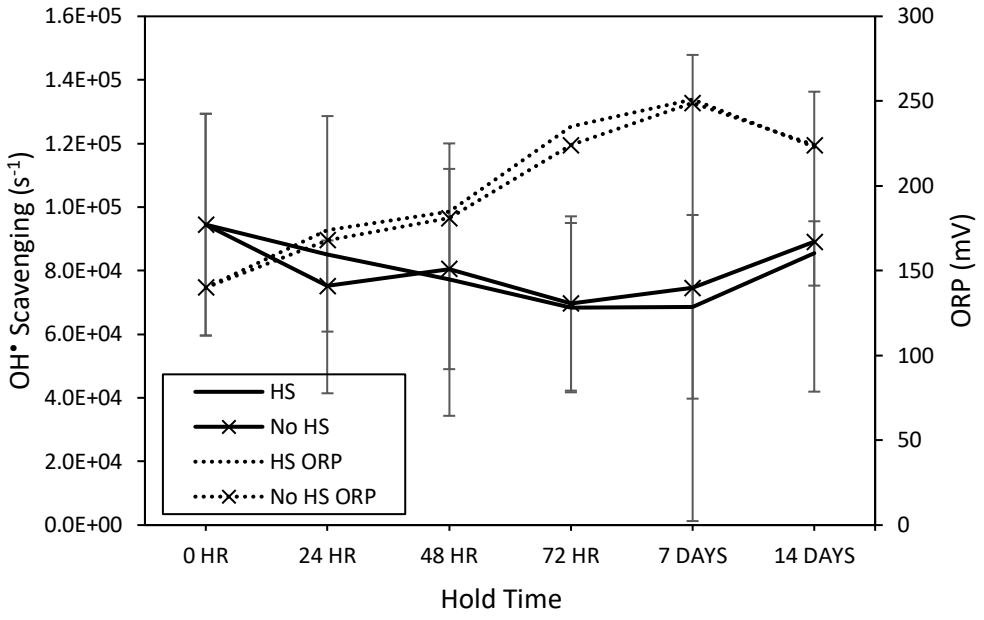

Figure 14: OH• Scavenging and ORP trends for Summer Concord samples over time

In Figure 15 for the Summer Concord samples, similar trends of negative correlation between scavenging and ORP are seen. During this season, ORP increased in storage over time while scavenging decreased after the 0 HR and remained low throughout the entire 14 days. After 7 days, ORP dropped significantly while scavenging increased significantly for both samples.

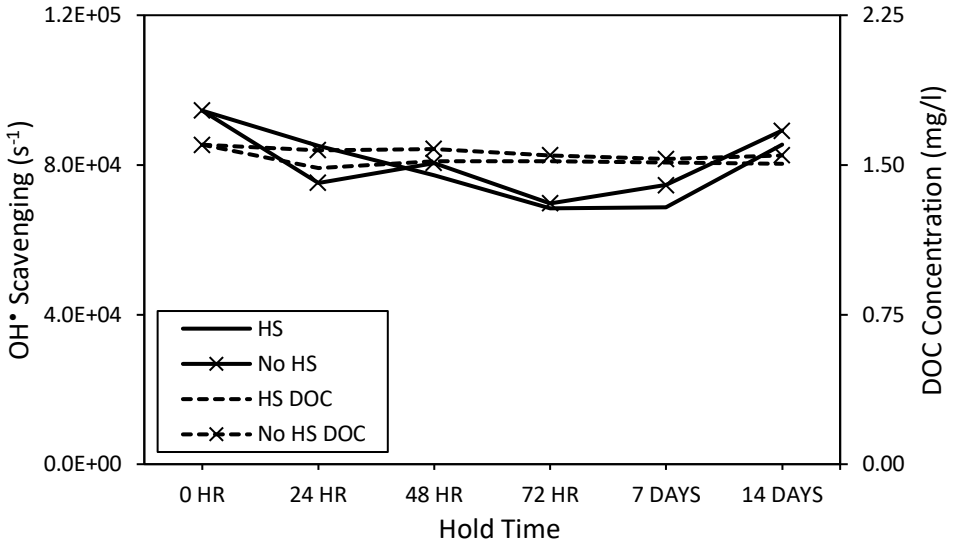

Figure 15: OH• Scavenging and DOC Concentration trends for Summer Concord samples over time

When comparing scavenging to DOC concentrations in Figure 16, DOC concentrations for both samples remained consistent throughout the entire 14 days. Concentrations stayed between 1.60 mg-C/l and 1.48 mg-C/l between both HS and no HS samples.

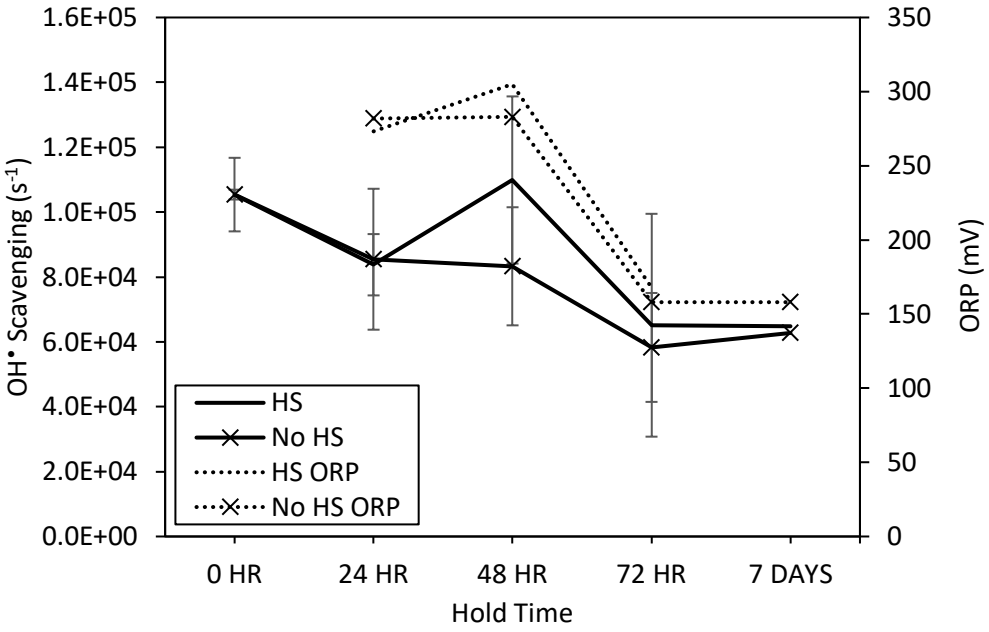

Figure 16: OH• Scavenging and ORP trends for Winter Mount Holly samples over time

For Mount Holly samples, scavenging and ORP are revealed to have positive correlations unlike the Concord samples. HS scavenging and no HS scavenging follows closely with their perspective ORP trends. As ORP increases, scavenging increases and as scavenging decreases, ORP decreases.

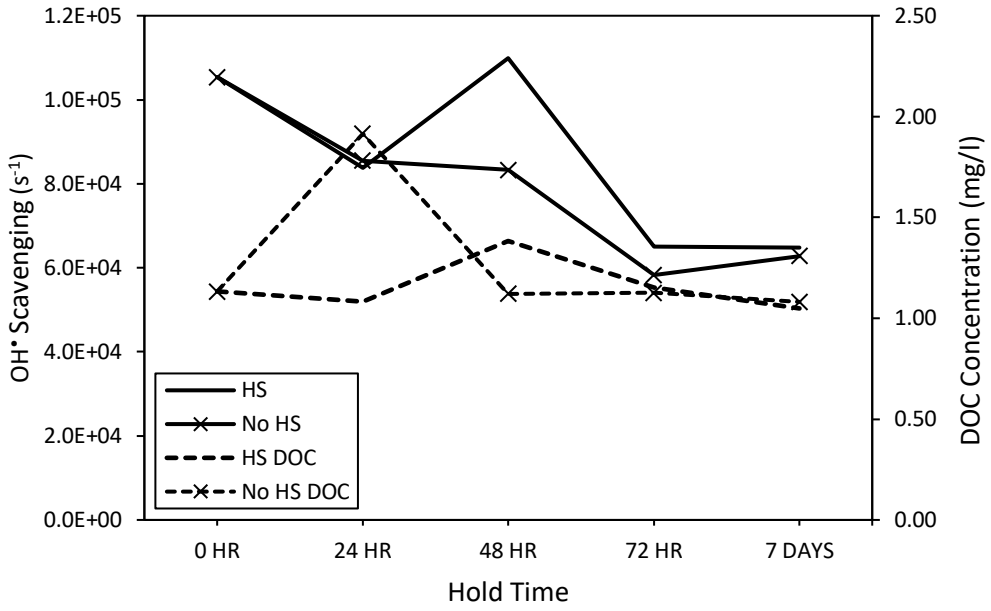

Figure 17: OH• Scavenging and DOC Concentration trends for Winter Mount Holly over time

In Figure 18, DOC concentration correlated positively within the HS samples, but revealed to be random within the no HS samples. Concentrations ranged from a maximum of 1.91 mg-C/l to a minimum of 1.05 mg-C/l between both HS and no HS samples.

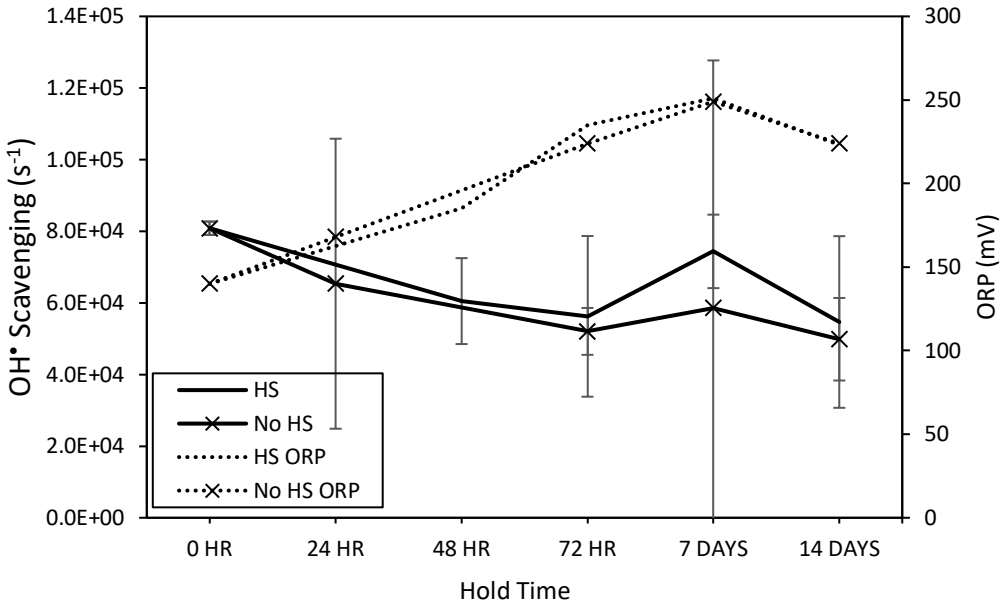

Figure 18: OH• Scavenging and ORP trends for Summer Mount Holly samples over time

In Figure 19, as ORP was consistently increasing during the first 72 hours in storage, scavenging simultaneously decreased. After 72 hours, as ORP continued to increase, the scavenging started to increase and positively correlated with ORP through 14 days of hold time. In Figure 20, DOC concentrations remained stable throughout the 14 days of hold time, only slightly decreasing from a maximum of 1.60 mg-C/l to a minimum of 1.50 mg-C/l for both HS and no HS samples.

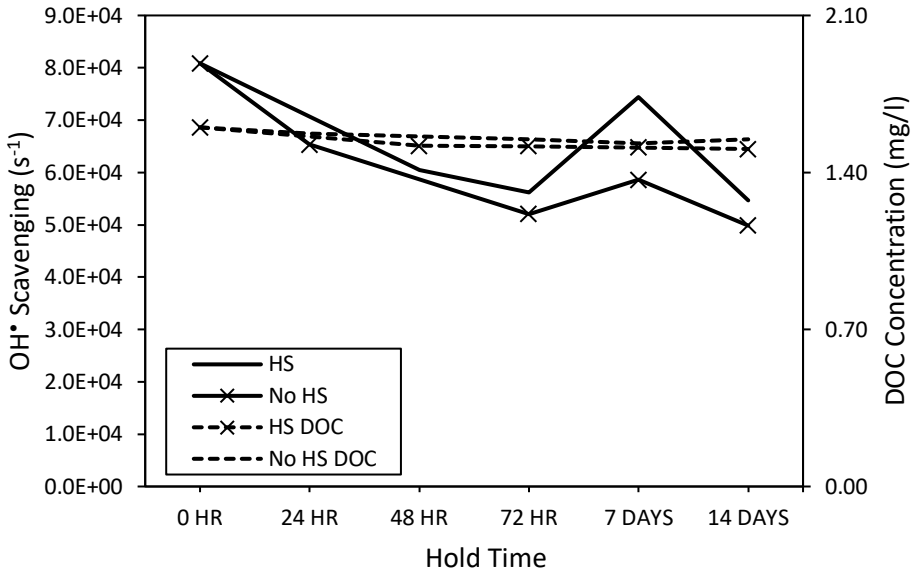

Figure 19: OH• Scavenging and DOC Concentration trends for Summer Mount Holly samples over time

4.7.5 ORP and OH• Scavenging Trends at Different Hold Times Discussion

Both Concord and Mount Holly samples revealed strong trends between scavenging and ORP. Whether it was negative or positive correlations, scavenging follows closely to how ORP was changing over time. For Concord samples, it was predominately a negative correlation between scavenging and ORP while Mount Holly revealed both strong positive and negative correlations interchangeably within the same sample over time.

While these relationships reveal the major influence of ORP on scavenging with some samples supporting hypothesis II, some samples did not. Hypothesis II states that as ORP increases under headspace conditions, scavenging is expected to decrease as the DOC has become more readily oxidized while in storage with headspace. The HS Winter Concord sample follows this relationship very closely, but the no HS Winter Concord

sample did not. Similarly, the HS Summer Concord sample follows a strong negative correlation between scavenging and ORP while the no HS Summer Concord also follows a negative correlation, although much weaker.

ORP between both storage conditions did not drift apart significantly but instead changed in the same pattern over time, however the HS ORP values were still slightly higher on average compared to no HS conditions. Oxygen present may have influenced the magnitude of these correlations that resulted in stronger correlations between the two variables whereas limited oxygen caused a weaker correlation in the no HS samples. The presence of oxygen may have allowed the dissolved organics to possibly change differently compared to limited oxygen, similarly how biochemical processes undergo in aerobic conditions versus anaerobic conditions in the environment. DOC biodegradation in the absence of oxygen has been shown to be lower due to thermodynamic constraints resulting in lower energy yield from microorganisms to break down substrates (Liu et al., 2020). Additionally, research have shown that 39.5% of DOM degraded under anaerobic conditions while 55.5% degraded under aerobic conditions (Lui et al., 2020) where this could explain the higher percentage of significant differences in OH scavenging in HS samples to initial samples compared to no HS scavenging. DOC composition is chemically and structurally diverse, where fractions within the complex composition can be more susceptible to biodegradation under specific conditions while other fractions are not (Liu et al., 2020).

Not only DOC varies chemically and structurally, but its composition also greatly depends on source and season, which may explain the differences in correlation between Concord and Mount Holly samples. For Winter Mount Holly samples, scavenging shows

a strong positive trend with ORP and for summer samples, scavenging and ORP started with strong negative correlations before revealing positive correlations.

Each sample extracts water from different lake reservoirs with unique ecosystems and biochemical processes. Seasonal DOC variability can be attributed by higher plant matter and decay during the winter months and microbial and algal processes during the summer months. Even through all these variabilities, scavenging within each sample nonetheless reveals strong correlations with ORP. Due to differences in correlations between the samples, it suggests that while ORP has a major influence on scavenging, other potential factors associated with DOC complexes might contribute to specific trends in scavenging that can dictate whether ORP will increase or decrease scavenging.

4.8 Analysis of DOC Rate Constants

The p-values between DOC rate constants in headspace and no headspace samples for each data set are summarized in this section. P-values were calculated using a t-Test. Table 14 summarizes the significant responses for Concord samples and Table 15 summarizes the responses for Mount Holly samples.

Table 13: P-values for Concord DOC Rate Constants between HS and no HS, $\alpha = 0.05$

	Data Set	P-value
Concord Winter	24 HS	0.027
	24 No HS	
	72 HS	0.065
	72 No HS	
Concord Summer	24 HS	0.035
	24 No HS	
	48 HS	0.957
	48 No Hs	
	72 HS	0.990
	72 No HS	
	7 Day HS	0.337
	7 Day No HS	
	14 HS	0.781
	14 No HS	

Table 14: P-values for Mt. Holly DOC Rate Constants between HS and no HS, $\alpha = 0.05$

	Data Set	P-value
Mt. Holly Winter	24 HS	0.0004
	24 No HS	
	48 HS	0.1809
	48 No HS	
	72 HR	0.0408
	72 No HS	
	7 HS	0.2522
	7 No HS	
Mt. Holly Summer	24 HS	0.0019
	24 No HS	
	48 HS	0.0014
	48 No HS	
	72 HS	0.0191
	72 No HS	
	7 Day HS	0.1340
	7 Day No HS	
	14 Day HS	0.0698
	14 Day No HS	

Table 14 summarizes the data set for Concord samples revealing significant differences between the DOC rate constants based on storage conditions within the 24 HR hold time for both seasons. All other hold times were non-significant, implying that rate constants stayed consistent within each hold time regardless of storage conditions. Table 15 summarizes the data set for Mount Holly samples, also revealing differences between the DOC rate constants within the 24 HR samples for both seasons with Mount Holly Summer additionally showing the 48 HR hold time as significant and both at 72 HR.

Table 16 and Table 17 summarizes the maximum, minimum, and average DOC rate constants in units of L mg-C^{-1} s^{-1} for each data set. The p-value for each table reveals the significance level in rate constants between seasons. For both sets, the rate constants are higher during in the winter samples compared to the summer samples. However, the difference is not statistically significant.

Concord Winter	Maximum	9.66×10^4
	Minimum	3.81×10^4
	Average	5.96×10^4
Concord Summer	Maximum	5.73×10^4
	Minimum	4.36×10^4
	Average	4.95×10^4
Concord Seasons p-value		0.401

Table 15: Concord DOC rate constants maximum, minimum, average and p-value significance

Mt. Holly Winter	Maximum	9.13×10^4
	Minimum	4.36×10^4
	Average	6.47×10^4
Mt. Holly Summer	Maximum	8.68×10^4
	Minimum	4.25×10^4
	Average	5.80×10^4
Mt. Holly Seasons P-value		0.368

Table 16: Mount Holly DOC rate constants maximum, minimum, average and p-value significance

Further analysis revealed a p-value for winter rate constants between Concord and Mount Holly of 0.679 and the p-value for summer of 0.141. The p-value between all Concord and Mount Holly rate constants is 0.0922. DOC rate constants reported from both sample sets were all higher than the reported values of 1.9 x 10^4 L mg-$C^{-1}s^{-1}$ (Goldstone et al., 2002) to 3 x 10^4 L mg-$C^{-1}s^{-1}$ (Westeroff et al., 1998) in literature.

4.7.4 DOC Rate Constant and ORP Correlation

The following figures plot DOC rate constants with ORP by source and season. HS samples are represented by square markets and no HS samples are represented by triangle markers.

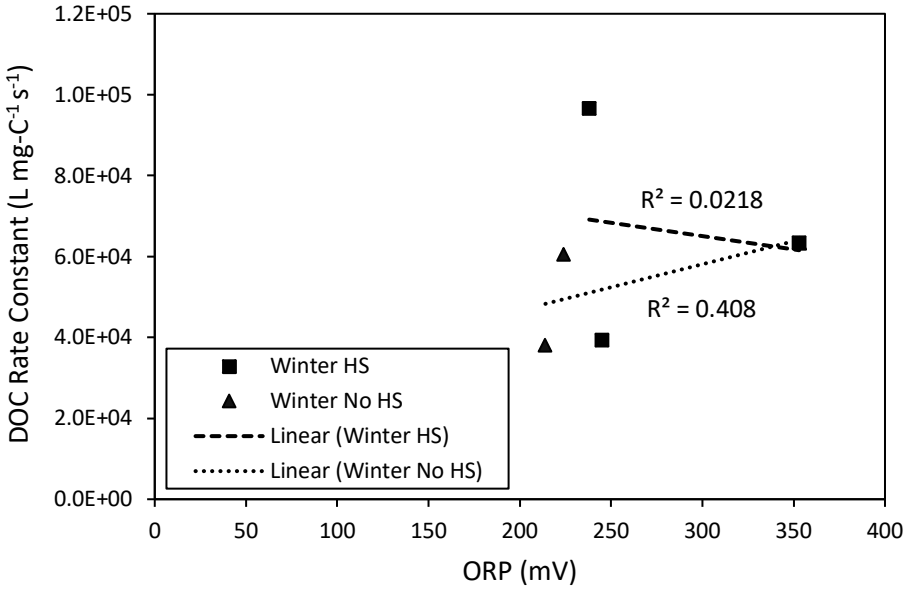

Figure 20: Correlation strength between ORP of water matrix and DOC Rate Constants for Concord Winter samples

This analysis evaluates whether the ORP of the water matrix influences the DOC rate constants with $OH^{\bullet}$. It is expected for rate constants to increase with lower ORP and decrease for higher ORP. In Figure 21, HS samples shows no correlation between DOC rate constants and ORP ($R^2 = 0.0218$) while no HS shows a relatively stronger relationship with an R^2 value of 0.408, however with only three data points this correlation may not be meaningful to conclude a direct relationship. No HS sample shows a slight increase in DOC rate constant with increasing ORP.

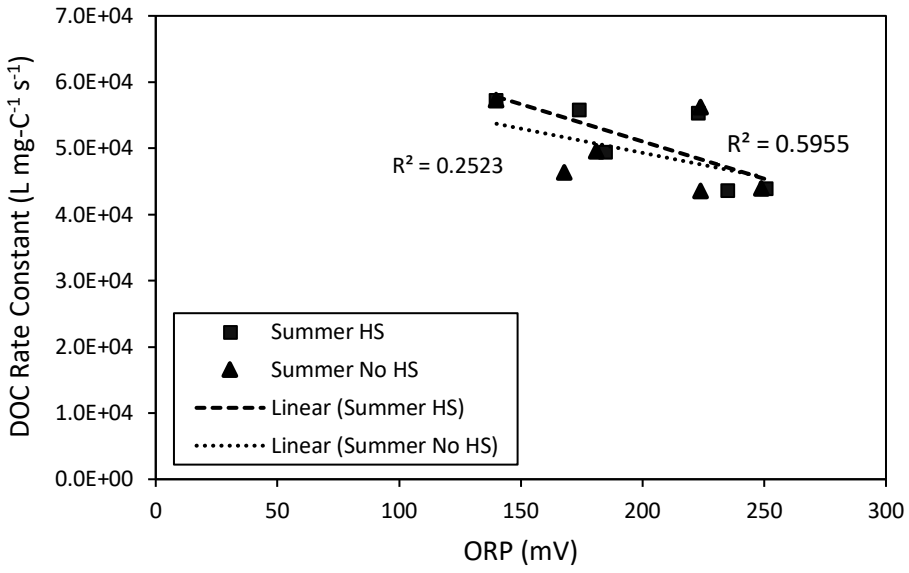

Figure 21: Correlation strength between ORP of water matrix and DOC Rate Constants for Concord Summer samples

In Figure 22, HS samples shows a strong relationship ($R^2 = 0.595$) and no HS shows a weaker relationship ($R^2 = 0.252$). Both correlations show DOC rate constants decreasing with increasing ORP. Both Concord samples each reveal two different correlations with ORP between seasonal samples which might suggest the influence of

other factors discussed in the previous section such as the DOC composition due to seasonal changes. Not only does DOC vary by composition, but DOC is further categorized based on the fractions that make up DOC such as recalcitrant, labile, active, and inactive (Hu et al., 2022). Fractions are based on the ratios of hydrogen to carbon atoms, and the molecular transformations the molecules have undergone (Hu et al., 2022). Based on DOC comprising of varying degrees of these fractions and the variability in rate constants in over 1,000 organic compounds analyzed by Buxton et al., (1987), the influence of ORP on DOC rate constants can possibly change uniquely from source to source.

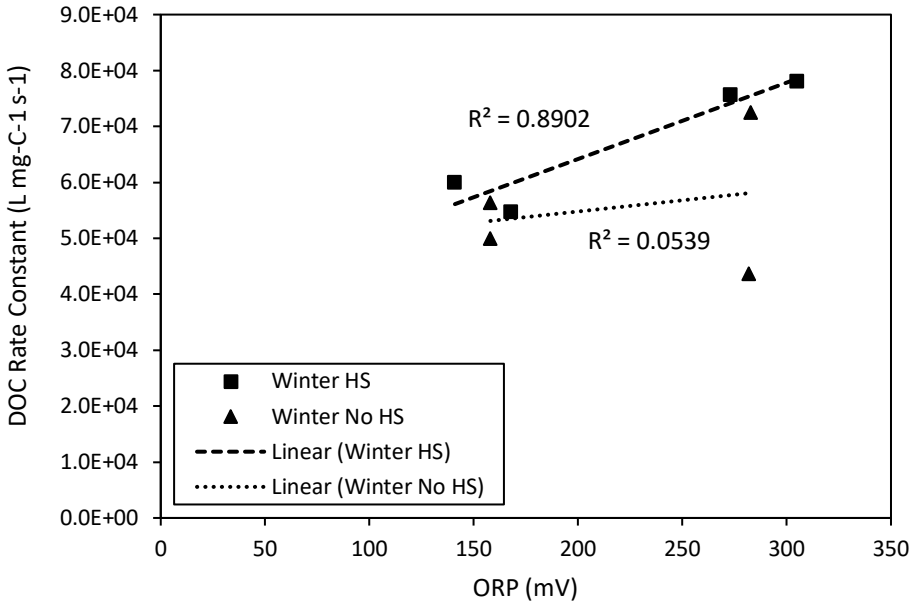

Figure 22: Correlation strength between ORP of water matrix and DOC Rate Constants for Winter Mount Holly Samples

In Figure 23, Winter samples shows a very strong ($R^2 = 0.8902$) positive relationship for the HS sample while no HS shows no relationship ($R^2 = 0.0539$)

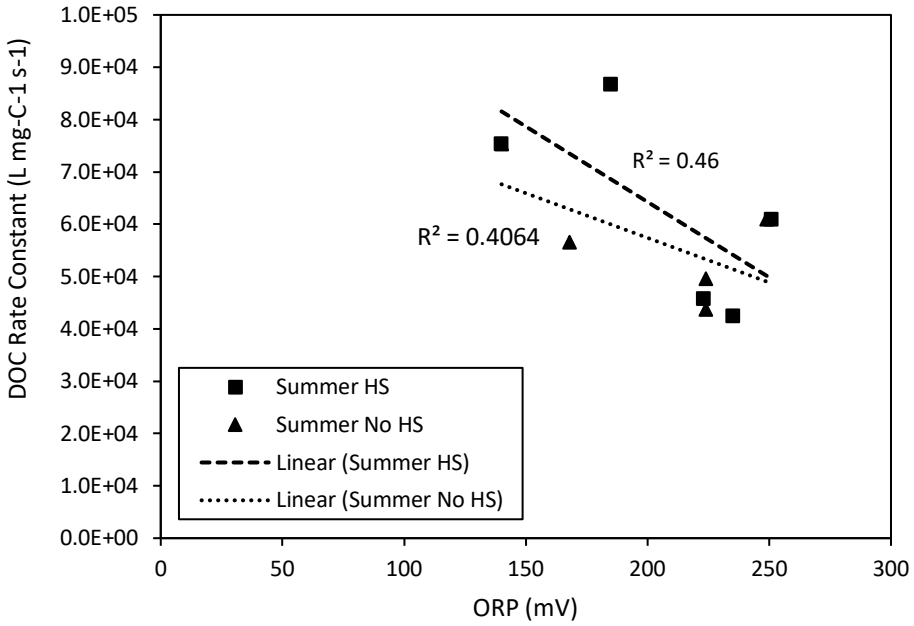

Figure 23: Correlation strength between ORP of water matrix and DOC Rate Constants for Summer Mount Holly samples

Both HS and no HS samples in Figure 24 show relatively strong relationships with R^2 values of 0.46 and 0.40 respectively. Similarly with Concord samples, the winter samples show an upward positive correlation while summer samples both reveal a downward negative correlation. Based on these consistent relationships, seasonal DOC changes could possibly be influencing how ORP oxidizes the organics that would impact both scavenging and the DOC rate constant in each sample.

Chapter 5: SUMMARY AND CONCLUSIONS

5.1 Summary

The goal of this study was to bridge the research gaps on the relationship between ORP and $OH^{\bullet}$ scavenging by organic matter, and ORP and DOC reaction rate constants with $OH^{\bullet}$. Additionally, this research analyzed the significance of the oxidation state of carbon in hundreds of organic compounds with their respective rate constants with $OH^{\bullet}$. It was hypothesized that 1.) the carbon oxidation state will influence reaction rates between organics and $OH^{\bullet}$, where the more reduced the state of carbon is, the higher the reaction rate constants and the more oxidized the state of carbon is, the lower the reaction rate is, and 2.) the ORP of the water matrix will influence $OH^{\bullet}$ scavenging by changing the redox state of DOM where reducing conditions will increase scavenging and oxidizing conditions will decrease scavenging. This research provided additional guidance on the testing of $OH^{\bullet}$ scavenging in AOPs, such as understanding how hold times and temperatures will affect $OH^{\bullet}$ scavenging and whether storage conditions play a role in reducing or increasing scavenging through ORP changes. Information on the impact of bisulfides and potassium permanganate on the testing of $OH^{\bullet}$ scavenging was also investigated.

5.2 Conclusions

Based on the statistical response for the analysis between the oxidation state of carbon and their respective reaction rate constants, there was a strong significant difference between the reaction rate constants of negative oxidation states of carbon and

positive oxidation states of carbon (p-value: 0.0000204, $\alpha = 0.05$) thus supporting hypothesis I.

Sample results show both negative and positive trends between ORP and $OH^{\bullet}$ scavenging over time, suggesting that ORP influences scavenging to a degree, however other potential factors to consider such as DOC composition (specific functional groups, chemical structures, and fractions) may also contribute to whether scavenging positively or negatively correlates with ORP. From the eight sets of samples analyzed for ORP and scavenging trends, Winter Concord HS and Summer Concord HS supports hypothesis II. Summer Concord No HS and both Summer Mount Holly HS and No HS weakly supports hypothesis II, and Winter Concord No HS and both Winter Mount Holly HS and No HS does not support hypothesis II. Overall, no sufficiently strong universal or local relationship between ORP and $OH^{\bullet}$ scavenging was determined.

Results shows significant differences in scavenging between the initial day of collection and at other various hold times, including 24 HR hold time samples, in 52% of all samples up to 14 days and therefore it is recommended to test for scavenging within a 24 HR hold time.

Under headspace and no headspace conditions, there were significant differences in scavenging in samples stored under both conditions meaning storage conditions do in fact change scavenging rates. Based on the hold time analysis, significant differences were seen across all samples under both storage conditions with 69% of headspace samples and 63% of no headspace samples being significantly different from the initial day. While there are significant changes in scavenging compared to the initial day, the storage conditions are not an important consideration in handling these samples.

Based on the temperature data, scavenging was significantly different (p-value = 0.039, $\alpha = 0.05$) for a sample at room temperature vs. for a refrigerated sample. Therefore, it is important to keep all samples at the same temperature during testing, and the temperature of the test sample should ideally represent the typical temperature of the water in the full-scale AOP system.

This research has provided additional information on bisulfides as the presence of sulfide compounds can be impact testing on reduced samples such as groundwater. Sulfide species are a potential major scavenger of $OH^{\bullet}$ with reaction rate constants of 1.5 x 10^{10} L mol^{-1} s^{-1} for hydrogen sulfide and 9.0 x 10^{9} L mol^{-1} s^{-1} for bisulfides (Buxton et al., 1987). Through this investigation, a molar absorption spectrum of bisulfides was determined. While it did not help to determine the identity of the unknown compound within the Mount Holly outliers, this data can be helpful for quickly identifying whether HS^{-} is likely to be present in a given water sample, especially for samples in a reduced state such as groundwater.

Potassium permanganate is widely used as a pre-oxidant in water treatment for the oxidation of iron and manganese, but information on the interferences from the residual with testing of scavenging is limited. During the $KMnO_4/H_2O_2$ study, there was a physical color change during the experiments as well as a small drop in H_2O_2 concentration that was approximately consistent with the expected drop based on stoichiometry of the reaction between these chemicals, and during the UV irradiation there was no observable decay of MB with 0.1 mg/L $KMnO_4$ present. Since $KMnO_4$ at this concentration still has distinctly visible pink color, it can be concluded that water that was preoxidized with $KMnO_4$ should not interfere with the measurement of scavenging

as long as there is no residual pink color present. As a result, it is recommended to test for scavenging with before pre-oxidation with $KMnO_4$ or with concentrations less than 0.1 mg/L.

5.3 Improvements

This research can provide the framework and the foundation to further investigate the influence of ORP and DOC changes on $OH^{\bullet}$ scavenging. The next steps would be to test samples with reduced (negative) ORP to allow changes over time to be more significant to understand the magnitude of influence ORP has on scavenging. ORP in this study were not significantly different between HS and no HS conditions and the range of ORP was relatively narrow, therefore testing of $OH^{\bullet}$ on reduced water samples and oxidized samples of significant differences can provide a better idea of the relationship between the variables.

Since DOC composition varies from source to source, testing of scavenging on a wide range of water samples from different sources might provide a better understanding on correlating universal trends in $OH^{\bullet}$ scavenging and ORP.

REFERENCES

1. Aeschbacher, M., Sander, M., & Schwarzenbach, R. (2010). Novel Electrochemical Approach to Assess the Redox Properties of Humic Substances, *Environmental Science & Technology, 44*(1), 87-93. DOI: 10.1021/es902627p

2. Arakaki, T., Anastasio, C., Kuroki, Y., Nakajima, H., Okada, K., Kotani, Y., Handa, D., Azechi, S., Kimura, T., Tsuhako, A., & Miyagi. Y. (2013). A General Scavenging Rate Constant for Reaction of Hydroxyl Radical with Organic Carbon in Atmospheric Waters, *Environmental Science & Technology, 47*(15), 8196-8203. DOI: 10.1021/es401927b

3. Bailey, K., and Taylor, G. (1937). The Retardation of Chemical Reactions. Part VII. The Reaction between Potassium Permanganate and Hydrogen Peroxide in Acid Solution. *Journal of the Chemical Society,* 994-999. DOI: 10.1039/JR9370000994

4. Bolton, J., Beck, S., &Linden, K. (2015). Protocol for the Determination of Fluence (UV Dose) Using A Low-Pressure or Low-Pressure High-Output UV Lamp in Bench-Scale Collimated Beam Ultraviolet Experiments, *IUVA News, 17*.

5. Bolton, J., & Linden, K. (2003). Standardization of Methods for Fluence (UV Dose) Determination in Bench-Scale UV Experiments, Journal of Environmental Engineering, 123(9). DOI: 10.1061/(ASCE)0733-9372(2003)129:3(209)

6. Boye, K., Noël, V., Tfaily, M., Bone, S., Williams, K., Bargar1, J., & Fendorf, S. (2017). Thermodynamically controlled preservation of organic carbon in floodplains, *Nature Geoscience, 10*, 415-417. DOI: 10.1038/ngeo2940

7. Brezonik, P. L., & Fulkerson-Brekken J. (1998). Nitrate-Induced Photolysis in Natural Waters: Controls on Concentrations of Hydroxyl Radical Photo-Intermediates by Natural Scavenging Agents, *Environmental Science & Technology, 32*(19), 3004-3010. DOI: 10.1021/es9802908

8. Buxton, V. G., Greenstock, L. C., Phillips Helman, P. W., Ross, B. A. (1987). Critical Review of rate constants for reactions of hydrated electrons, hydrogen atoms and hydroxyl radicals (·OH/·O−) in Aqueous Solution, *Journal of Physical and Chemical Reference Data, 17*, 513-886. DOI: 10.1063/1.555805.

9. Deng, Y., Zhao, R. (2015). Advanced Oxidation Processes (AOPs) in Wastewater Treatment. *Curr Pollution Rep, 1*, 167–176. DOI: 10.1007/s40726-015-0015-z

10. Dong, M. M., Mezyk, P. S., & Rosario-Ortiz, L. F. (2010). Reactivity of Effluent Organic Matter (EfOM) with Hydroxyl Radical as a Function of Molecular Weight, *Environmental Science & Technology, 44*(15), 5714-5720. DOI: 10.1021/es1004736

11. Dick, J., Yu, M., Tan, J., & Lu., A. (2019). Changes in Carbon Oxidation State of Metagenomes Along Geochemical Redox Gradients, *Frontiers in Microbiology, 10*(120). DOI: 10.3389/fmicb.2019.00120

12. Glaze, W., Lay, Y., & Kang, J. (1995). *Industrial & Engineering Chemistry Research, 34*(7), 2314-2323. DOI: 10.1021/ie00046a013

13. Gligorovski, S., Strekowski, R., Barbati, S., & Vione, D. (2015). Environmental Implications of Hydroxyl Radicals ($OH^{\bullet}$), *Chemical Reviews, 115*(24), 13051-13092. DOI: 10.1021/cr500310b

14. Goldstone, J. V., M. J. Pullin, S. Bertilsson, & B. M. Voelker. (2002). Reactions of hydroxyl radical with humic substances: Bleaching, mineralization, and production of bioavailable carbon substrates, *Environmental Science & Technology*, *36*(3), 364–372. DOI: 10.1021/es0109646

15. Hu, A., Jang, K., Meng, F., Stegen, J., Tanentzap, A., Choi, M., Lennon, J., Soininen, J., and Wang, J. (2022). Microbial and Environmental Processes Shape the Link between Organic Matter Functional Traits and Composition, *Environmental Science and Technology,* 56*(14),* 10504-10516. DOI: 10.1021/acs.est.2c01432

16. Kane, E. S., Veverica, T. J., Tfaily, M. M., Lilleskov, E. A., Meingast, K. M., Kolka, R. K., et al. (2019). Reduction-oxidation potential and dissolved organic matter composition in northern peat soil: Interactive controls of water table position and plant functional groups, *Journal of Geophysical Research: Biogeosciences, 124,* 3600–3617. DOI: 10.1029/2019JG005339

17. Keiluweit, M., Nico, P., Kleber, M., & Fendorf, S. (2016). Are oxygen limitations under recognized regulators of organic carbon turnover in upland soils? *Biogeochemistry, 127*, 157–171. DOI 10.1007/s10533-015-0180-6

18. Klassen, N., Marchington, D., & McGowan, H. (1994). H_2O_2 Determination by the I3-Method and by KMnO4 Titration, *Analytical Chemistry, 66*(18), 2921-2925. DOI: 10.1021/ac00090a020

19. Kroll, J. H., Donahue, N. M., Jimenez, J. L., Kessler, S. H., Canagaratna, M. R., Wilson, K. R., Altieri, K. E., Mazzoleni, L. R., Wozniak, A. S., Bluhm, H., Mysak, E. R., Smith, J. D., Kolb, C. E., & Worsnop, D. R. (2011). Carbon oxidation state as a metric for describing the chemistry of atmospheric organic aerosol. *Nature chemistry, 3*(2), 133–139. DO1: 10.1038/nchem.948

20. LaRowe, E. D., & Cappellen, V. P. (2011). Degradation of natural organic matter: A thermodynamic analysis, *Geochimica et Cosmochimica Acta, 75*(8)*,* 2030-2042. DOI: 10.1016/j.gca.2011.01.020

21. Li, Xican. (2013). Solvent effects and improvements in the deoxyribose degradation assay for hydroxyl radical-scavenging, *Food chemistry, 141*(3)*,* 2083–2088. DOI: 10.1016/j.foodchem.2013.05.084

22. Liu, J., Liang, J., Bravo, A., Wei, S., Yang, C., Wang, D., and Jiang, Tao. (2021). Anaerobic and aerobic biodegradation of soil-extracted dissolved organic matter from the water-level-fluctuation zone of the Three Gorges Reservoir region, China. *Science of the Total Environment*, 764, 142857. DOI: 10.1016/j.scitotenv.2020.142857

23. Peng, X., Gai, S., Cheng, K., Yang, F. (2022). Roles of humic substances redox activity on environmental remediation, *Journal of Hazardous Materials, 435,* 129070. DOI: 10.1016/j.jhazmat.2022.129070

24. Sarathy, S., Stefan, M., Royce, A., & Mohseni, M. (2011). Pilot-scale UV/H2O2 advanced oxidation process for surface water treatment and downstream biological treatment: effects on natural organic matter characteristics and DBP formation potential, *Environmental Technology, 32*(15), 1709-1718. DOI: 10.1080/09593330.2011.553843

25. Sharp, E., Parsons, S., Jefferson., B. (2006). Seasonal variations in natural organic matter and its impact on coagulation in water treatment, *Science of the Total Environment, 363*, 183-194. DOI: 10.1016/j.scitotenv.2005.05.032

26. Snoeyink, V., & Jenkins, D. (1980). Water Chemistry, *John Wiley & Sons,* 135. ISBN: 0-471-051969-9

27. Souza, B., Dantas, R., Cruz, A., Sans, C., Esplugas, S., & Dezotti, M. (2014). Photochemical oxidation of municipal secondary effluents at low H2O2 dosage: Study of hydroxyl radical scavenging and process performance, *Chemical Engineering Journal, 237,* 268–276. DOI: 10.1016/j.cej.2013.10.025

28. Stern, N., Mejia, J., He, S., Yang, Y., Ginder-Vogel, M., and Roden, E. (2018). Dual Role of Humic Substances As Electron Donor and Shuttle for Dissimilatory Iron Reduction, *Environmental Science & Technology, 52*(10) 5691-5699. DO1: 10.1021/acs.est.7b06574

29. US Environmental Protection Agency. (2021). Field Measurement of Oxidation-Reduction Potential, *epa.gov.* Retrieved September 9, 2022 from https://www.epa.gov/quality/field-measurement-oxidation-reduction-potential

30. Westerhoff, P., Aiken, G., Amy, G., & Debroux, J. (2011). Relationships between the structure of natural organic matter and its reactivity towards molecular ozone and hydroxyl radicals, *Water Research, 33*(10), 2265-2276. DOI: 10.1016/S0043-1354(98)00447-3

31. Xu, X., Chen, C., Lee, D., Wang, A., Guo, W., Zhou, X., Guo, H., Yuan, Y., Ren, N., and Chang, J. (2013). Sulfate-reduction, sulfide-oxidation an elemental sulfur bioreduction process: Modeling and experimental validation. *Bioresource Technology,* 147, 202-211. DOI: 10.1016/j.biortech.2013.07.113

32. Yang, S., Guo, Z., Miao, F., Xue, Q., & Qin, S. (2010). The hydroxyl radical scavenging activity of chitosan, hyaluronan, starch and their O-carboxymethylated derivatives, *Carbohydrate Polymers, 82*(4), 1043-1045. DOI: 10.1016/j.carbpol.2010.06.014

APPENDIX

Winter Concord		Initial	HS		No HS	
Hold Times		0 HR	24 HR	72 HR	24 HR	72 HR
Bicarbonate Alkalinity		0.00046	0.00034	0.000117	0.00032	0.000293
Temperature (°C)		13.8	16.6	14.4	16.6	14.8
pH (s.u.)		7.32	6.85	6.76	6.84	6.84
Average Absorbance with H_2O_2						
UV Dose (mJ/cm^2)	0	0.409	0.394	0.386	0.417	0.393
	100	0.333	0.359	0.301	0.321	0.288
	200	0.269	0.302	0.220	0.258	0.207
	300	0.217	0.261	0.164	0.210	0.149
	400	0.175	0.215	0.119	0.168	0.109
	500	0.140	0.185	0.086	0.132	0.080
Average Absorbance without H_2O_2						
UV Dose (mJ/cm^2)	0	0.390	0.368	0.384	0.386	0.390
	100	0.409	0.366	0.383	0.381	0.385
	200	0.398	0.364	0.380	0.378	0.383
	300	0.382	0.361	0.376	0.376	0.380
	400	0.380	0.360	0.376	0.375	0.378
	500	0.378	0.358	0.373	0.373	0.375
[MB] at Initial Absorbance		1.10E-06	1.06E-06	1.04E-06	1.12E-06	1.06E-06
Lamp Irradiance (W/cm^2)		2.30E-03	1.99E-03	1.94E-03	1.99E-03	1.94E-03

Summer Concord		Initial	HS				
Hold Times		0 HR	24 HR	48 HR	72 HR	7 DAYS	14 DAYS
Bicarbonate Alkalinity		0.000329	0.0001236	0.000266	0.000263	0.00027	0.000258
Temperature (°C)		22.6	14.3	14.4	12.7	13.3	11.7
pH (s.u.)		7.19	7.11	7.26	6.89	7.17	7.8
Average Absorbance with H_2O_2							
UV Dose (mJ/cm^2)	0	0.327	0.340	0.361	0.368	0.370	0.365
	100	0.271	0.274	0.301	0.288	0.274	0.289
	200	0.231	0.223	0.244	0.225	0.213	0.233
	300	0.192	0.180	0.201	0.175	0.164	0.187
	400	0.163	0.145	0.162	0.137	0.130	0.151
	500	0.135	0.119	0.131	0.106	0.100	0.123
Average Absorbance without H_2O_2							
UV Dose (mJ/cm^2)	0	0.334	0.350	0.363	0.372	0.370	0.365
	100	0.327	0.344	0.361	0.369	0.367	0.362
	200	0.315	0.342	0.358	0.367	0.366	0.359
	300	0.313	0.340	0.356	0.365	0.364	0.357
	400	0.311	0.339	0.355	0.363	0.363	0.355
	500	0.309	0.337	0.346	0.360	0.362	0.353
[MB] at Initial Absorbance		8.78E-07	9.14E-07	9.74E-07	9.89E-07	9.92E-07	9.80E-07
Lamp Irradiance (W/cm^2)		2.03E-03	2.17E-03	2.20E-03	2.70E-03	2.14E-03	2.30E-03

Summer Concord		No HS				
Hold Times		24 HR	48 HR	72 HR	7 DAYS	14 DAYS
Bicarbonate Alkalinity		0.000253	0.000266	0.000264	0.000258	0.00025
Temperature (°C)		14.6	14.4	12.7	13.4	11.7
pH (s.u.)		7.09	7.18	6.95	7.16	7.52
Average Absorbance with H_2O_2						
UV Dose (mJ/cm^2)	0	0.347	0.361	0.369	0.372	0.358
	100	0.275	0.301	0.293	0.368	0.287
	200	0.219	0.249	0.232	0.366	0.234
	300	0.173	0.205	0.183	0.365	0.195
	400	0.139	0.169	0.145	0.364	0.162
	500	0.113	0.140	0.114	0.363	0.135
Average Absorbance Without H_2O_2						
UV Dose (mJ/cm^2)	0	0.341	0.361	0.362	0.330	0.351
	100	0.337	0.358	0.358	0.331	0.348
	200	0.336	0.355	0.356	0.329	0.346
	300	0.335	0.353	0.355	0.328	0.345
	400	0.332	0.352	0.352	0.328	0.343
	500	0.332	0.350	0.351	0.328	0.341
[MB] at Initial Absorbance		9.32E-07	9.68E-07	9.91E-07	1.00E-06	9.60E-07
Lamp Irradiance (W/cm^2)		2.17E-03	2.20E-03	2.27E-03	2.14E-03	2.30E-03

Winter Mount Holly		Initial	HS			
Hold Times		0 HR	24 HR	48 HR	72 HR	7 DAYS
Bicarbonate Alkalinity		0.000234	0.000234	0.000216	0.000236	0.000216
Temperature (°C)		19.9	17.4	13.5	14	14.8
pH (s.u.)		6.85	7.45	7.7	7.33	7.34
Average Absorbance with H_2O_2						
UV Dose (mJ/cm^2)	0	0.372	0.380	0.375	0.392	0.381
	100	0.300	0.302	0.291	0.285	0.285
	200	0.234	0.235	0.239	0.211	0.210
	300	0.190	0.180	0.195	0.157	0.158
	400	0.156	0.137	0.162	0.115	0.116
	500	0.128	0.111	0.133	0.091	0.086
Average Absorbance Without H_2O_2						
UV Dose (mJ/cm^2)	0	0.372	0.379	0.388	0.393	0.372
	100	0.368	0.377	0.387	0.387	0.370
	200	0.368	0.373	0.384	0.385	0.366
	300	0.367	0.370	0.382	0.383	0.364
	400	0.366	0.368	0.380	0.380	0.363
	500	0.364	0.366	0.379	0.377	0.359
[M] at Initial Absorbance		9.99E-07	1.02E-06	1.01E-06	1.05E-06	1.02E-06
Lamp Irradiance (W/cm^2)		2.20E-03	2.90E-03	2.80E-03	2.60E-03	2.40E-03

Winter Mount Holly		No HS			
Hold Times		24 HR	48 HR	72 HR	7 DAYS
Bicarbonate Alkalinity		0.000236	0.000235	0.00024	0.000217
Temperature (°C)		17.5	17.5	13.3	14.8
pH (s.u.)		7.56	7.62	7.47	7.38
Average Absorbance with H_2O_2					
UV Dose (mJ/cm^2)	0	0.375	0.380	0.390	0.364
	100	0.263	0.285	0.385	0.273
	200	0.224	0.216	0.383	0.199
	300	0.176	0.171	0.380	0.147
	400	0.136	0.130	0.378	0.105
	500	0.109	0.109	0.375	0.079
Average Absorbance without H_2O_2					
UV Dose (mJ/cm^2)	0	0.390	0.390	0.369	0.357
	100	0.379	0.387	0.372	0.353
	200	0.375	0.386	0.372	0.349
	300	0.372	0.383	0.372	0.345
	400	0.369	0.381	0.371	0.344
	500	0.367	0.379	0.372	0.343
[M] at Initial Absorbance		1.01E-06	1.02E-06	1.06E-06	9.77E-07
Lamp Irradiance (W/cm^2)		2.90E-03	2.48E-03	2.60E-03	2.40E-03

Summer Mount Holly		Initial	HS				
Hold Times		0 HR	24 HR	48 HR	72 HR	7 DAYS	14 DAYS
Bicarbonate Alkalinity		0.000246	0.000262	0.000254	0.000247	0.000254	0.00025
Temperature (°C)		24.9	14.7	9.2	11	12.3	11.9
pH (s.u.)		7.26	7.27	7.31	7.84	7.33	7.36
Average Absorbance with H_2O_2							
UV Dose (mJ/cm^2)	0	0.372	0.359	0.370	0.350	0.378	0.347
	100	0.288	0.334	0.281	0.347	0.276	0.255
	200	0.242	0.312	0.217	0.344	0.210	0.190
	300	0.207	0.290	0.165	0.343	0.175	0.141
	400	0.145	0.270	0.129	0.342	0.138	0.104
	500	0.115	0.252	0.100	0.341	0.110	0.077
Average Absorbance without H_2O_2							
UV Dose (mJ/cm^2)	0	0.360	0.342	0.360	0.330	0.348	0.336
	100	0.357	0.340	0.357	0.331	0.343	0.329
	200	0.349	0.338	0.353	0.329	0.342	0.327
	300	0.347	0.335	0.352	0.328	0.337	0.325
	400	0.344	0.333	0.352	0.328	0.335	0.324
	500	0.341	0.331	0.351	0.328	0.333	0.320
[M] at Initial Absorbance		9.97E-07	9.65E-07	9.93E-07	9.98E-07	1.01E-06	9.32E-07
Lamp Irradiance (W/cm^2)		2.36E-03	2.30E-03	2.40E-03	2.40E-03	2.39E-03	2.80E-03

Summer Mount Holly		No HS				
Hold Times		24 HR	48 HR	72 HR	7 DAYS	14 DAYS
Bicarbonate Alkalinity		0.00026	0.000244	0.000238	0.000248	0.000238
Temperature (°C)		14.3	9.5	11.1	12.3	11.8
pH (s.u.)		7.24	7.43	7.92	7.34	7.26
Average Absorbance with H_2O_2						
UV Dose (mJ/cm^2)	0	0.338	0.376	0.365	0.374	0.366
	100	0.246	0.352	0.279	0.286	0.272
	200	0.211	0.331	0.210	0.225	0.205
	300	0.163	0.310	0.159	0.175	0.156
	400	0.126	0.292	0.121	0.139	0.119
	500	0.101	0.275	0.093	0.108	0.090
Average Absorbance without H_2O_2						
UV Dose (mJ/cm^2)	0	0.327	0.353	0.343	0.372	0.333
	100	0.324	0.350	0.338	0.368	0.332
	200	0.321	0.349	0.333	0.366	0.329
	300	0.319	0.348	0.330	0.365	0.328
	400	0.316	0.347	0.328	0.364	0.326
	500	0.314	0.347	0.326	0.363	0.324
[M] at Initial Absorbance		9.10E-07	1.01E-06	9.77E-07	1.00E-06	9.83E-07
Lamp Irradiance (W/cm^2)		2.30E-03	2.40E-03	2.40E-03	2.39E-03	2.80E-03